The Extractable Power from Tidal Streams, including a Case Study for Haida Gwaii

by

Justin Burns Blanchfield
B.Eng., Carleton University, 2004

A Thesis Submitted in Partial Fulfillment of the Requirements for the Degree of

MASTER OF APPLIED SCIENCE

in the Department of Mechanical Engineering

University of Victoria

Supervisory Committee

The Extractable Power from Tidal Streams, including a Case Study for Haida Gwaii

by

Justin Burns Blanchfield
B.Eng., Carleton University, 2004

Supervisory Committee

Dr. Andrew Rowe, Department of Mechanical Engineering
Supervisor

Dr. Peter Wild, Department of Mechanical Engineering
Supervisor

Dr. Chris Garrett, Department of Physics and Astronomy
Outside Member

Dr. Aaron Gulliver, Department of Electrical and Computer Engineering
External Member

Supervisory Committee

Dr. Andrew Rowe, Department of Mechanical Engineering
Supervisor

Dr. Peter Wild, Department of Mechanical Engineering
Supervisor

Dr. Chris Garrett, Department of Physics and Astronomy
Outside Member

Dr. Aaron Gulliver, Department of Electrical and Computer Engineering
External Member

Abstract

Interest is growing worldwide among utility companies and governments of maritime countries in assessing the power potential of tidal streams. While the latest assessment for Canadian coastlines estimates a resource of approximately 42 GW, these results are based on the average kinetic energy flux through the channel. It has been shown, however, that this method cannot be used to obtain the maximum extractable power for electricity generation. This work presents an updated theory for the extractable power from a channel linking a bay to the open ocean. A mathematical model is developed for one-dimensional, non-steady flow through a channel of varying cross-section. Flow acceleration, bottom drag, and exit separation effects are included in the momentum balance. The model is applied to Masset Sound and Masset Inlet in Haida Gwaii, a remote island region, to determine the extractable power and its associated impacts to the tidal amplitude and volume flow rate through the channel.

Table of Contents

Supervisory Committee ..... **ii**

Abstract ..... **iii**

Table of Contents ..... **iv**

List of Figures ..... **vi**

Nomenclature ..... **viii**

Acknowledgments ..... **x**

Chapter 1 Introduction **1**

1.1 Background 2
1.2 Tidal Stream Power Resource Assessment 4
1.3 Thesis Objective 11
1.4 Thesis Outline 11

Chapter 2 Tidal Stream Power Model **12**

2.1 Governing Equation 13
2.2 Continuity 22
2.3 Power Equations 24
2.4 Summary 27

Chapter 3 Results and Discussion **28**

3.1 Negligible Bottom Drag and Exit Separation Effects 29
3.1.1 Linear Drag – Analytic Solution 29
3.1.2 Quadratic Drag – Numerical Solution 34
3.1.3 Validation 36
3.2 Including Bottom Drag and Separation Effects - Quadratic Drag 38
3.2.1 Maximum Extractable Power 39
3.2.2 Validation 40
3.2.3 Determining Bay Geometry Term and Loss Parameter 42
3.3 Summary 46

Chapter 4 Masset Sound Case Study 47

4.1 Introduction 47
4.2 Tidal Regime 47
4.3 Determining the Bay Geometry Term and Loss Parameter 49
4.3.1 Method #1 – Bathymetric Data and Amplitude Ratio 49
4.3.2 Method #2 – Amplitude Ratio and Phase Lag 53
4.5 Extractable Power 56
4.6 Tidal Regime Perturbation 59

Chapter 5 Conclusions and Recommendations 60

5.1 Conclusions 60
5.2 Recommendations 62

References 64

Appendices 69

Appendix A – Negligible Bottom Drag and Exit Separation Effects - Linear Drag 69
Appendix B – Including Bottom Drag and Exit Separation Effects - Quadratic Drag 73
Appendix C – Helmholtz Frequency 75

List of Figures

Figure 2.1: Schematic drawing of a channel linking a bay to the open ocean..... 12

Figure 3.1: Phase lag as a function of the turbine drag parameter for varying bay geometries when drag is assumed to be linear with the volume flow rate. 31

Figure 3.2: Non-dimensional average extractable power as a function of the turbine drag parameter for varying bay geometries when friction is assumed linearly proportional with the flow rate and losses are negligible. 33

Figure 3.3: Relative power as a function of the turbine drag parameter for varying bay geometries when friction is assumed linearly proportional with the flow rate and losses are negligible. 33

Figure 3.4: Non-dimensional average extractable power as a function of the turbine drag parameter for varying bay geometries when drag is assumed to be quadratic with the flow rate and losses are negligible. 35

Figure 3.5: Relative power as a function of the turbine drag parameter for varying bay geometries when drag is assumed to be quadratic with the flow rate and losses are negligible. 36

Figure 3.6: Non-dimensional average extractable power for linear and quadratic drag cases when $\beta = 0$ and losses are assumed negligible. 37

Figure 3.7: Maximum non-dimensional average extractable power as a function of the loss parameter for varying bay geometries when drag is assumed to be quadratic with the flow rate. 39

Figure 3.8: Multiplier as a function of the loss parameter for varying bay geometries when drag is assumed to be quadratic with the flow rate. 40

Figure 3.9: Maximum non-dimensional average extractable power for $\beta = 0$ as a function of the loss parameter. 41

Figure 3.10: Amplitude ratio as a function of the loss parameter for varying bay geometries when drag is assumed to be quadratic with the flow rate 44

Figure 3.11: Phase lag as a function of the loss parameter for varying bay geometries when drag is assumed to be quadratic with the flow rate 44

Figure 3.12: Light line represents various values of the amplitude ratio (in italic). Dark line represents various values of phase lag in degrees (in bold). Contours are a function of the loss parameter and the bay geometry term. 45

Figure 4.1: Masset Sound on Graham Island in Haida Gwaii [24]. 48

Figure 4.2: CHS tidal predictions for Wiah Point and Port Clements [11]. 48

Figure 4.3: Masset Inlet [25]. 51

Figure 4.4: Masset Sound [25]. 51

Figure 4.5: Digitized soundings for Masset Sound. 52

Figure 4.6: Maximum non-dimensional flow rate as a function of the loss parameter for a bay defined by β = 1.45. 56

Figure 4.7: Non-dimensional average extractable power as a function of the turbine drag parameter for Masset Sound when defined by $\beta = 1.45$ and $\lambda_0^* = 8$. 58

Figure 4.8: Power multiplier as a function of the loss parameter for Masset Sound as defined by $\beta = 1.45$. 58

Nomenclature

a	amplitude of dominant tidal constituent outside channel in open ocean [m]
A	surface area of bay [m^2]
c	channel geometry term [m^{-1}]
C_d	bottom drag coefficient
E	cross-sectional area of channel [m^2]
E_L	cross-sectional area at the ends of the channel [m^2]
E_{turb}	cross-sectional area of a turbine
F	resistance force [ms^{-2}]
F_{turb}	turbine drag [ms^{-2}]
g	acceleration due to gravity [ms^{-2}]
h	water depth [m]
L	channel length [m]
n_1	dependence of turbine drag on flow rate
n_2	dependence of bottom drag on flow rate
p	pressure [Nm^{-2}]
P	power [Nms^{-1}]
Q	volume flow rate through channel [m^3s^{-1}]
Q_0	maximum flow rate in undisturbed state [m^3s^{-1}]
t	time [s]
u	flow velocity [ms^{-1}]
u_L	flow velocity at end of channel [ms^{-1}]
u_{L0}	maximum flow velocity at end of channel in the undisturbed state [ms^{-1}]
x	Cartesian coordinate

Greek Letters

β	bay geometry term
λ_1	turbine drag parameter
λ_2	bottom drag parameter
λ_0	loss parameter [m^{-4}]
λ	sum of the turbine drag parameter and the loss parameter [m^{-4}]
ρ	density of sea water [kgm^{-3}]
ω	frequency of dominant tidal constituent outside channel in open ocean [s^{-1}]
ω_n	natural frequency of the bay and channel [s^{-1}]
ζ	water surface elevation [m]
ζ_{Bay}	water surface elevation in the bay [m]
ζ_0	water surface elevation just outside the channel in the open ocean [m]

Superscripts

*	non-dimensional value

Subscripts

avg	average
max	maximum

Abbreviations

CHS	Canadian Hydrographic Service
VDFVP	Viscously damped forced vibration problem

Acknowledgments

There are several people who I would like to sincerely thank. While some of you may not read much further than this page, trust that you have been pivotal in the successful completion of this thesis.

I cannot possibly thank my parents, Burke and Arlene Blanchfield, enough. Life can *flow* quite smoothly when you receive the constant love and support that only proud parents can offer.

Thank you Tim Warren, John Kinahan, and Tim Robillard, for introducing me to the wonder and excitement of mathematics, physics, healthy living, and skiing recklessly fast! You provided me with great insight during my most formative years.

Stephanie Kelly has supported me from the very beginning. She has watched this work grow and provided endless encouragement. Thank you for your love, support, and respect.

It has been extremely rewarding to study under my supervisors and mentors: Dr. Andrew Rowe, Dr. Peter Wild, Dr. Chris Garrett, and Dr. Lawrence Pitt. They provided just the right amount of support, encouragement, and wisdom along the way. You have inspired me in many ways and taught me the value of independent researching skills. Thank you for your assistance in turning a ski bum into an effective researcher; we are almost half way there!

To my fellow graduate students, Gwynn Elfring, Jesse Maddaloni, and Matt Schuett; thank you for your support and sincere interest in this work. You provided many insightful comments when they were needed most.

Chapter 1

Introduction

While the development of tidal stream energy is still in its infancy, interest continues to grow worldwide in assessing its true potential [1-4]. This interest is driven by the desire for energy supply security and concerns with the environmental impacts of fossil fuel combustion. As a result, there has been continued development in the theory behind the accurate assessment of this resource [5-8]. Tidal streams may have the potential to provide significant amounts of electricity for coastal and remote island communities. As fossil fuel resources continue to be depleted, the rising costs associated with conventional power generation using diesel, natural gas, and coal may promote the economic development of renewable energy technologies, such as tidal energy conversion devices. It is, therefore, essential to accurately quantify the extractable power from tidal streams to optimize electricity generation and provide reliable power predictions.

While the latest assessment for Canadian coastlines estimates a resource potential of approximately 42 GW, these results are based on the kinetic energy flux through the most constricted cross-section of a channel in the undisturbed state [2]. Here, the term *undisturbed* describes the natural state prior to installing tidal stream energy converters. This method has no rigorous scientific basis for tidal streams and cannot be related to the maximum extractable power [5, 6]. This work presents modifications to the model presented by Garrett and Cummins [5] to extend the

theory of the extractable power of a tidal stream in a channel linking a bay to the open ocean.

It is necessary for the reader to have a basic understanding of how tidal currents are generated in the earth's oceans. The following section provides a brief explanation of the physics involved.

1.1 Background

Ocean tides are primarily generated due to the gravitational forces of the sun and the moon. These tide-generating gravitational forces are inversely proportional to the cube of the distance between the center of the earth and the center of the sun and moon, respectively. While the moon has 27 million times less mass than the sun, it is 390 times closer to the earth, making it the dominant tide-generating force. Since a lunar day is 24 hours and 50 minutes, the tides generated by the moon produce two local high tides every lunar day [9].

The largest tidal ranges, or difference in magnitude between the low and high tide, are created when the moon and sun are aligned with the earth. Known as spring tides, the gravitational forces of the sun and moon are additive. A new moon is produced when the moon is directly between the earth and the sun, whereas a full moon is produced when the moon is on the opposite side of the earth. Neap tides produce the minimum tidal ranges and occur when the moon is at a right angle to the sun relative to the earth [9].

The generation of the tides is quite complicated, however, since the earth's axis of rotation is tilted to the plane of its orbit around the sun. In addition, the plane of the moon's orbit is tilted to the plane of the earth's orbit around the sun. These tilts cause the angle of declination of the moon, or the angle between the positions of the moon relative to the earth's equator, to vary throughout the tidal cycle. The result is a difference in magnitude between the two successive high or low tides due to the declination of both the sun and moon. This difference is referred to as the diurnal inequality [9].

The distances between the earth and the moon, and between the earth and the sun, also plays a role in the magnitude of the tidal range since the gravitational forces are a function of the distance cubed. These variables, along with almost 400 other periodic tide-generating forces, commonly referred to as tidal constituents, must be considered when predicting a local tidal regime. Depending on the location, a relatively accurate prediction, however, may be based on only eight of the major constituents [9, 10].

The observable tides in many parts of the world are generally classified as either a diurnal or semidiurnal tide. Diurnal tides have a single high and low tide each lunar day, whereas semidiurnal tides have two high and two low tides each lunar day with similar successive high and low tides. A mixed tide is a combination of the two and is strongly affected by the diurnal inequality. Successive high and low tides are, therefore, significantly different in mixed tides [9].

The Canadian Hydrographic Service (CHS) has closely monitored the tidal regimes along Canadian coastlines. Water gauges measure the water surface elevation over a prescribed length of time. A harmonic analysis is then applied to determine the magnitude and phase of the tidal constituents with known frequencies. CHS has accumulated an extensive database of tidal constituents for Canadian coastlines [11].

Tidal currents are shallow-water waves resulting from the horizontal displacement of the ocean waters. A tidal stream capable of producing significant amounts of power may be found in a channel linking a bay to the open ocean or in a channel connecting two large basins, such as flow between an island and the mainland. As the tidal flow travels through these constricted passages, the flow speed increases, making them potentially feasible for large scale power generation [5, 6].

1.2 Tidal Stream Power Resource Assessment

Historically, the energy flux method has been the primary method for estimating the resource potential of a tidal stream [1-4]. This method assumes that the extractable power is directly proportional to the kinetic energy flux through the most constricted cross-section of the channel in the undisturbed state. The head difference across the channel is assumed to have a negligible impact. For an isolated turbine, the extractable power is assumed to be some fraction of the instantaneous kinetic energy flux upstream of the turbine, defined as

$$Energy\ flux = \frac{1}{2}\rho E_{turb} u^3, \tag{1.1}$$

where ρ is the density of water, E_{turb} is the cross-sectional area of the turbine, and u is the instantaneous depth-averaged upstream current velocity. The classic result, given by Betz [12, 13] and Lanchester [14], limits the extractable power from the turbine to 59% of the upstream energy flux, excluding mechanical and electrical efficiencies. This Lanchester-Betz limit, however, assumes frictionless, incompressible, steady flow with negligible heat transfer and shaft work, and neglects drag from support structures. The applicability to real channels is, therefore, limited when extracting a significant fraction of the total kinetic energy flux through the channel.

Since tidal current energy is intermittent and reaches its maximum output for only a fraction of the year, the average power is often quoted within resource assessments. The *average extractable power* is calculated by averaging the instantaneous power over the tidal cycle.

In a report prepared by Triton Consultants Ltd. [2], the tidal stream energy resource for Canadian coastlines was assessed. Based on the energy flux method, Triton acknowledges that the extractable power is only loosely related to the kinetic energy flux. Triton, as well as many other resource assessments [3, 15-17] define the instantaneous extractable power in the form

$$P = \frac{1}{2} N \eta \rho E_{turb} u^3, \tag{1.2}$$

where N is the number of turbines and η is the turbine efficiency. Assumptions for these scaling values vary widely. The number of installed turbines is limited by construction issues related to water depth and inter-unit wake considerations [1].

A report produced by Black and Veatch [3] for the Carbon Trust, provided a resource assessment for the UK, Europe, and the world. This paper presented a literature review of all the major resource assessments that had been done independently prior to 2004. The report highlights three major contributions for the UK resource assessment [15-17] Each independent report based their estimations on the energy flux method, similar to that presented by Triton [1, 2]. Assumptions were made for turbine efficiencies, availability, turbine density (the number of turbines that can fit in an area), cut-in, and cut-off velocities. In [16], the current velocity is assumed to *fully* recover between rows of turbines when appropriately spaced, thereby assuming that extracting power from tidal streams would have negligible impacts on the downstream flow speed. These papers [1, 2, 15-17] also predict the maximum extractable power based on the maximum spring tide flow velocity, which only actually occurs for a fraction of the year.

Resource assessments for Europe and global tidal streams are also listed in Black and Veatch [3]; all are based on the energy flux method with various assumptions. It is apparent that the scope of these assumptions limits the validity of the energy flux method.

Black and Veatch [3] develop their own method for resource assessment based on its literature review, entitled the *Flux Method*. This method incorporates the two dominant tidal constituents to model a velocity distribution for the tidal cycle. While this method is still only based on the kinetic energy flux in the undisturbed state, it acknowledges that the extractable power will vary over the tidal cycle. Black and Veatch [3] introduce a significant impact factor, representing the percentage of the energy flux that may be extracted without significant economic and environmental impacts. A value of 20% was assumed as a preliminary estimate with little explanation or scientific basis.

Black and Veatch [3] quickly refer to the work of Bryden and Melville [8] which states that, “The nature of this resource and how effectively to exploit it has not been adequately accepted outside the small active tidal research and development community”. Bryden and Melville [8] derive a limit for the extractable power of a simple hypothetical channel linking two infinite oceans, as 10% of the undisturbed kinetic energy flux. This analysis is based on a simple uniform channel of constant cross-sectional area and volume flow rate, neglecting dynamical effects resulting from the time variation of the water elevation within the momentum balance. While these assumptions limit its applicability to real channels, Bryden and Melville [8] as well as Bryden and Couch [7], do introduce the important idea that only a fraction of the undisturbed energy flux may actually be extractable from tidal streams.

Bryden and Melville [8] conclude that selecting potential sites for extracting tidal energy is not a simple case of identifying areas with large peak tidal current. They stress the fact that the energy flux method is flawed in its assumption that local tidal regimes will not be significantly altered by power extraction.

It is apparent from the aforementioned literature, that resource assessments based on the energy flux method do not accurately predict the extractable power of a tidal stream. While many researchers have attempted to quantify the actual extractable power by assigning a scaling value to the undisturbed energy flux through the channel, little progress had been made in assessing the maximum value of this fraction in real channels.

Garrett and Cummins [5] took a novel approach and began exploring the effects of installing isolated turbines within a channel linking a bay to the open ocean. Based on a momentum balance, they showed that an array of isolated turbines allow flow to divert around them, inducing downstream mixing, resulting in additional power losses. They suggest that the maximum power may be extracted only with uniformly distributed turbines across the entire cross-section of the channel, thus minimizing free flow around them. Garrett and Cummins [5] conclude that a few installed turbines will have little impact on most tidal streams; however, little power will be generated. The addition of more turbines will produce greater amounts of power but will also impede the flow and hence have a negative feedback on the power generated.

Garrett and Cummins [5] quantify the maximum extractable power from a channel linking a bay to the open ocean as

$$P_{avg} = 0.24\rho g A \omega a^2, \tag{1.3}$$

where g is the acceleration due to gravity, A is the surface area of the bay, and a and ω are the amplitude and frequency of the dominant tidal constituent just outside the channel in the open ocean, respectively. This analysis neglects mechanical and electrical inefficiencies, drag on supporting structures, and assume that the drag associated with installed turbines is quadratic in the flow velocity. This one-dimensional model neglects flow acceleration, bottom drag, and exit separation effects. The exit of the channel may be at either end of the channel where the flow exits to the bay or open ocean, depending on which way the tides are flowing. A general conclusion is that the extractable power has no simple relationship with the energy flux in the undisturbed state.

A more sophisticated model was developed by Garrett and Cummins [6] for a channel of varying cross-sectional area linking two large basins, such as a channel between an offshore island and the mainland. This one-dimensional model, derived from a momentum balance includes flow acceleration, bottom drag, and exit separation effects. The two large basins are assumed to have their own independent tidal regimes, unaffected by the flow through the channel. A general result is that the maximum extractable power, averaged over the tidal cycle, is approximately equal to

$$P_{avg} = 0.22\rho g a Q_0 , \tag{1.4}$$

where Q_0 is the maximum flow rate in the undisturbed state and a is the amplitude of the sea level difference between the ends of the channel.

If bottom drag is much less important than separation effect, Garrett and Cummins [6] concluded that the maximum average extractable power may be written as

$$P = 0.38\left(\frac{1}{2}\rho E_L \overline{|u_{L0}|^3}\right), \tag{1.5}$$

where u_{L0} is the flow velocity at any instant at the end of the channel in the undisturbed state. Equation (1.5) is similar to the kinetic energy flux with a reduction factor of 0.38, however, it must be evaluated at the exit of cross-sectional area, E_L, which may not be the most constricted part of the channel.

1.3 Thesis Objective

The present work uses the model developed by Garrett and Cummins [6] to extend the analysis presented in Garrett and Cummins [5] by including bottom drag, exit separation effects, and flow acceleration within the dynamical balance. This updated one-dimensional model effectively describes the flow through a channel, of varying cross-sectional area, linking a bay to the open ocean. The associated impacts on the flow regime are quantified for varying levels of power extraction. A case study for Masset Sound and Masset Inlet, in Haida Gwaii, is analyzed to validate the model and estimate the extractable power.

1.4 Thesis Outline

This thesis begins by developing the model for flow through a channel connecting a bay to the open ocean. The governing equations for the flow through the channel are derived from a momentum balance and continuity. The average extractable power is then derived as a function of the volume flow rate through the channel and the water surface elevation just outside the channel in the open ocean. The governing equation, continuity, and power equations are left in a generalized form. Modelling results and a thorough discussion are then presented based on alternative assumptions for the flow. An extensive case study for Masset Sound and Masset Inlet, in Haida Gwaii is analyzed, followed by general conclusions and recommendations for future work.

Chapter 2

Tidal Stream Power Model

A mathematical model is developed for a tidal stream in a channel linking a bay to the open ocean. The model solves for the flow rate, Q, and the water surface elevation within the bay, ζ_{Bay}, as a function of time, *t*, given a bay surface area, *A*, and channel cross-sectional area, *E(x)*, which may vary along the length of the channel, *L*. The water surface elevation just outside the channel in the open ocean, ζ_0, is assumed to be unaffected by the flow through the channel. Here, *water surface elevation* refers to the height above or below the average tide height. A schematic drawing for this model is presented in Figure 2.1. The momentum balance, continuity, and power equations are derived and presented in their general forms. This is convenient as it will allow for multiple solutions based on alternative assumptions. These solutions will be discussed in Chapter 3.

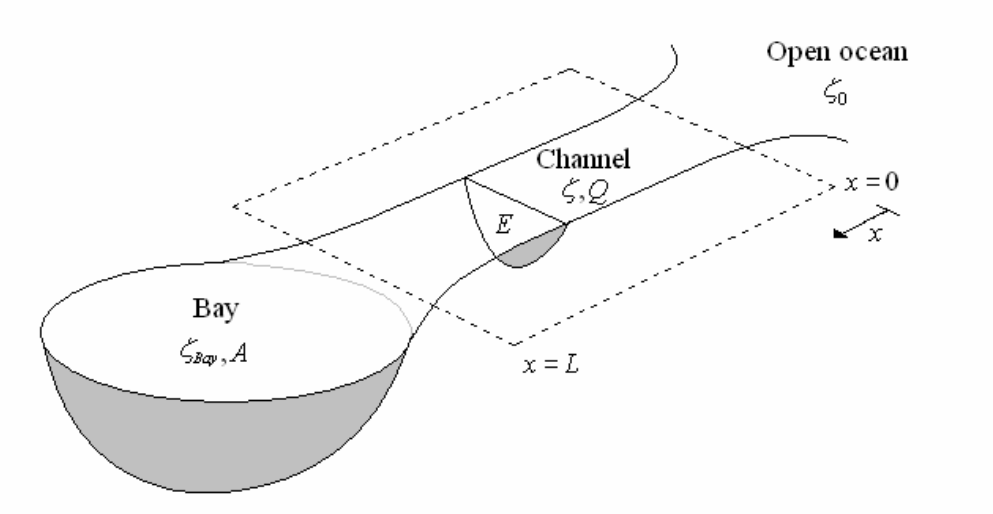

Figure 2.1: Schematic drawing of a channel linking a bay to the open ocean.

2.1 Governing Equation

The governing equations for the flow through a channel linking a bay to the open ocean are derived from momentum balance and continuity. For a viscous, incompressible, and Newtonian fluid, the momentum balance reduces to the Navier-Stokes equation. For a one-dimensional flow along the *x*-axis, Navier-Stokes may be written as

$$-\frac{\partial p(x,t)}{\partial x}-\rho F(x,t)=\rho\left(\frac{\partial u(x,t)}{\partial t}+u(x,t)\frac{\partial u(x,t)}{\partial x}\right), \tag{2.1}$$

where $F(x,t)$ represents the resistance forces per unit mass of sea water within the channel. The resistance forces may include bottom drag and turbine drag associated with power generation. The flow velocity is represented as $u(x,t)$, ρ is the density of sea water, and $p(x,t)$ is pressure.

The first term in equation (2.1) represents the hydrostatic pressure gradient and may be expressed as

$$\frac{\partial p(x,t)}{\partial x}=\rho g\frac{\partial \zeta(x,t)}{\partial x}, \tag{2.2}$$

where g is the acceleration due to gravity, and $\zeta(x,t)$ is the water surface elevation along the channel. The change in water surface elevation along the length of the

channel, $\partial\zeta/\partial x$, provides the pressure gradient required to drive the flow in and out of the bay with the flood and ebb tides, respectively.

To maximize power extraction, turbines must be deployed such that all the flow passes through them. Isolated turbines allow some of the flow to divert around them, inducing downstream lateral motion and mixing, leading to increased power losses within the channel. Garrett and Cummins [6] have suggested deploying uniform "fences" of turbines across the cross-sectional area of the channel [6]. While installing uniform "fences" of turbines may be impractical in engineering terms, the assumption significantly simplifies the analysis and provides insight into the maximum extractable power from the tidal steam.

The one-dimensional flow assumption implies that the resistance forces and flow velocity are independent of the cross channel position and only vary along the length of the channel. We assume that the cross-sectional area of the channel and the surface area of the bay are unaffected by the rise and fall of the tides, as for flow at low Froude number and with a tidal range which is not a significant fraction of the water depth.

Substituting equation (2.2) into equation (2.1),

$$-F = \frac{\partial u}{\partial t} + u\frac{\partial u}{\partial x} + g\frac{\partial \zeta}{\partial x}. \tag{2.3}$$

The resistance forces are, therefore, proportional to the sum of the local acceleration, $\partial u/\partial t$, the convective acceleration, $u\left(\partial u/\partial x\right)$, and the water surface elevation gradient, $\partial \zeta /\partial x$.

Integrating equation (2.3) over the entire length of the channel,

$$-\int_0^L F dx = \int_0^L \frac{\partial u}{\partial t} dx + \int_0^L u \frac{\partial u}{\partial x} dx + g \int_0^L \frac{\partial \zeta}{\partial x} dx . \tag{2.4}$$

Assuming that the tidal wavelength is much longer than the channel length and that the surface area of the bay is much larger than the surface area of the channel, volume conservation implies that the volume flux is independent of position and may be expressed only as a function of time as

$$Q(t) = Eu , \tag{2.5}$$

where E is the local cross-sectional area of the channel.

Based on this assumption, the local acceleration term may then be written as

$$\int_0^L \frac{\partial u}{\partial t} dx = \int_0^L \frac{1}{E} \frac{\partial Q}{\partial t} dx = \frac{\partial Q}{\partial t} \int_0^L \frac{1}{E} dx . \tag{2.6}$$

The channel geometry term, c, is now introduced and defined as

$$c = \int_0^L E^{-1} dx \,. \tag{2.7}$$

Substituting equation (2.7) into equation (2.6), the local acceleration term is

$$\int_0^L \frac{\partial u}{\partial t} dx = c \frac{\partial Q}{\partial t} \,. \tag{2.8}$$

If the cross-sectional area of the channel is assumed to be constant along its entire length, the channel geometry term is

$$c = \frac{L}{E} \,. \tag{2.9}$$

The flow is assumed to be drawn in smoothly at the channel entrance from a region with a large surface area, weak currents, and a prescribed tidal elevation [6]. The convective acceleration term, therefore, describes the flow separation at the end of the channel and may be written as a function of the flow rate as

$$\int_0^L u \frac{\partial u}{\partial x} dx = \frac{1}{2} u_L \left| u_L \right| = \frac{1}{2E_L^2} Q \left| Q \right| , \tag{2.10}$$

where E_L represents the local cross-sectional area at the end of the channel. Since the model solves for both the flood and ebb tide, symmetry is implied. The cross-sectional areas at either end of the channel are assumed the same.

The change in water surface elevation along the channel, is

$$\int_0^L \frac{\partial \zeta}{\partial x} dx = \zeta_{Bay} - \zeta_0 , \tag{2.11}$$

where ζ_{Bay} is the water surface elevation within the bay and ζ_0 represents the water surface elevation just outside the channel in the open ocean. Substituting equations (2.11), (2.10), and (2.8) into equation (2.4), the momentum balance for the flow through the channel is

$$c\frac{dQ}{dt} = g\left(\zeta_0 - \zeta_{Bay}\right) - \int_0^L F dx - \frac{1}{2E_L^2} Q|Q| . \tag{2.12}$$

The resistance force per unit mass of water, *F*, representing the bottom drag within the channel and turbine drag associated with potential power generation, is defined as

$$\int_0^L F dx = \int_0^L F_{turb}\, dx + \int_0^L \frac{C_d}{h} u^{n_2} dx , \tag{2.13}$$

where $\int_0^L F_{turb}\,dx$ represents the turbine drag, $\int_0^L \frac{C_d}{h} u^{n_2}\,dx$ represents the bottom drag, C_d is the bottom drag coefficient, and *h(x)* is the water depth [6, 18].

The bottom drag is expressed as a function of the flow rate as

$$\int_0^L \frac{C_d}{h} u|u|^{n_2-1}\,dx = \lambda_2 Q|Q|^{n_2-1}, \tag{2.14}$$

where the bottom drag parameter is defined as

$$\lambda_2 = \int_0^L C_d (hE^{n_2})^{-1}\,dx\,. \tag{2.15}$$

The turbine drag is expressed as a function of the flow rate as

$$\int_0^L F_{turb}\,dx = \lambda_1 Q|Q|^{n_1-1}, \tag{2.16}$$

where λ_1 is related to the number of turbines and their location along the channel, and will be referred to as the turbine drag parameter.

The relationship between drag and the flow rate, defined by n_1 and n_2, are left arbitrary at this point. The drag is linearly proportional to the flow rate when

$n_1 = n_2 = 1$ and quadratic when $n_1 = n_2 = 2$. Both linear and quadratic drag laws will be explored later in this thesis. The turbine drag and bottom drag, however, will be assumed to have the same dependence on the flow rate (ie. $n_1 = n_2 = n$).

Substituting equations (2.16) and (2.14) into equation (2.13), the total drag within the channel is

$$\int_0^L F dx = \lambda_1 Q|Q|^{n_1 - 1} + \lambda_2 Q|Q|^{n_2 - 1}. \tag{2.17}$$

Substituting equation (2.17) into equation (2.12), the governing equation is

$$c\frac{dQ}{dt} = g(\zeta_0 - \zeta_{Bay}) - \lambda_1 Q|Q|^{n_1 - 1} - \lambda_2 Q|Q|^{n_2 - 1} - \frac{1}{2E_L^2} Q|Q|. \tag{2.18}$$

Non-dimensional analysis eliminates the need for site specific parameters and reduces the number of variables. The governing equation may be written in its non-dimensional form by first dividing both sides of the equation by the acceleration due to gravity, *g*, and the amplitude of the dominant tidal constituent, *a*, just outside the channel in the open ocean of frequency, ω. The resulting expression is as follows:

$$\frac{c}{ga}\frac{dQ}{dt} = \frac{\zeta_0}{a} - \frac{\zeta_{Bay}}{a} - \frac{\lambda_1}{ga} Q|Q|^{n_1 - 1} - \frac{\lambda_2}{ga} Q|Q|^{n_2 - 1} - \frac{1}{2}\frac{1}{gaE_L^2} Q|Q|. \tag{2.19}$$

The non-dimensional water surface elevation is

$$\zeta^* = \frac{\zeta}{a}, \tag{2.20}$$

and non-dimensional time is defined as

$$t^* = \omega t\,. \tag{2.21}$$

Substituting equations (2.21) and (2.20) into equation (2.19),

$$\frac{c\omega}{ga}\frac{dQ}{dt^*} = \zeta_0^* - \zeta_{Bay}^* - \frac{\lambda_1}{ga}Q\left|Q\right|^{n_1-1} - \frac{\lambda_2}{ga}Q\left|Q\right|^{n_2-1} - \frac{1}{2}\frac{1}{gaE_L^2}Q\left|Q\right|. \tag{2.22}$$

The non-dimensional flow rate is defined as

$$Q^* = \frac{c\omega}{ga}Q, \tag{2.23}$$

and is substituted into equation (2.22), yielding,

$$\begin{aligned}\frac{dQ^*}{dt^*} = \zeta_0^* - \zeta_{Bay}^* - \lambda_1\frac{(ga)^{n_1-1}}{(c\omega)^{n_1}}Q^*\left|Q^*\right|^{n_1-1} - \lambda_2\frac{(ga)^{n_2-1}}{(c\omega)^{n_2}}Q^*\left|Q^*\right|^{n_2-1} \\ -\frac{1}{2}\frac{ga}{(c\omega E_L)^2}Q^*\left|Q^*\right|.\end{aligned} \tag{2.24}$$

The non-dimensional turbine drag parameter and bottom drag parameter are defined as

$$\lambda_1^* = \lambda_1 \frac{(ga)^{n_1-1}}{(c\omega)^{n_1}}, \tag{2.25}$$

and

$$\lambda_2^* = \lambda_2 \frac{(ga)^{n_2-1}}{(c\omega)^{n_2}}, \tag{2.26}$$

respectively. Substituting equations (2.25) and (2.26) into equation (2.24), the non-dimensional momentum balance for the flow through the channel is

$$\begin{aligned} \frac{dQ^*}{dt^*} = \zeta_0^* - \zeta_{Bay}^* - \lambda_1^* Q^* \left|Q^*\right|^{n_1-1} - \lambda_2^* Q^* \left|Q^*\right|^{n_2-1} \\ - \frac{ga}{2(c\omega E_L)^2} Q^* \left|Q^*\right|. \end{aligned} \tag{2.27}$$

Continuity is now applied to determine the relationship between the water surface elevation within the bay and the flow rate through the entrance.

2.2 Continuity

Continuity states that the mass within the system is conserved. The water surface elevation within the bay may be expressed as a function of the flow rate through the channel and the surface area of the bay as

$$\frac{d\zeta_{Bay}}{dt} = \frac{Q}{A}. \tag{2.28}$$

We assume that the tides rise and fall uniformly within the bay, as for a bay with a horizontal scale much less than the tidal wavelength.

As the surface area of the bay increases toward infinity, the dependence of the water surface elevation in the bay on the flow rate through the channel approaches zero. For this reason, Garrett and Cummins [6] neglected this dependence when modelling the extractable power from a channel connecting two large basins.

In the present analysis, the general case of a channel connecting a bay to the open ocean will be examined. This general case effectively describes both scenarios presented in [5] and [6], since the surface area may equal any positive value greater than zero. The model will solve the bay scenario for any value of surface area greater than zero, while a channel connecting two large basins is described as the surface area approaches infinity.

Substituting equations (2.20), (2.21), and (2.23) into equation (2.28) the non-dimensionalized continuity equation is

$$\frac{d\zeta_{Bay}^{*}}{dt^{*}} = \frac{g}{cA\omega^{2}} Q^{*}. \tag{2.29}$$

To eliminate the dimensional values in equation (2.29), a bay geometry term is defined as

$$\beta = \frac{g}{cA\omega^{2}}. \tag{2.30}$$

and substituted into equation (2.29), yielding

$$\frac{d\zeta_{Bay}^{*}}{dt^{*}} = \beta Q^{*}. \tag{2.31}$$

The governing equation (2.27) and continuity (2.31) are solved simultaneously to determine the flow rate and water surface elevation within the bay for varying levels of turbine drag, bottom drag, exit separation effects, and open ocean tidal amplitude as a function of time. The relationship between drag and the flow rate is left in its general form. Equations (2.27) and (2.31) represent a coupled, first-order, non-linear, non-homogeneous ordinary differential equation system. Once the system of equations is solved, the extractable power from the channel may be calculated as a function of the flow rate. The power equations are now derived.

2.3 Power Equations

The *total* extracted power over the entire channel, P, includes power extracted from the channel due to bottom drag and the power extracted for electricity generation using tidal stream energy converters. At any given instant during the tidal cycle, the total power may be defined as [6]

$$P = \rho Q \int_0^L F dx \,. \tag{2.32}$$

The *average* extractable power for electricity generation over a tidal cycle, as indicated by the overbar, is then

$$P_{avg} = \rho Q \overline{\int_0^L F_{turb} dx} \,. \tag{2.33}$$

Substituting equation (2.16) into equation (2.33),

$$P_{avg} = \rho \lambda_1 \overline{Q^2 |Q|^{n_2 - 1}} \,. \tag{2.34}$$

Substituting equations (2.23) and (2.25) into equation (2.34),

$$P_{avg} = \rho \frac{(ga)^2}{c\omega} \lambda_1^* \overline{Q^{*2} |Q^*|^{n_1 - 1}} \,. \tag{2.35}$$

The non-dimensional average extractable power for electricity generation is

$$P_{avg}^{*} = \lambda_1^{*} \overline{Q^{*2} \left| Q^{*} \right|^{n_1 - 1}} , \tag{2.36}$$

where the dimensional average extractable power is

$$P_{avg} = P_{avg}^{*} \frac{\rho (ga)^2}{c\omega} . \tag{2.37}$$

It was shown in [6] that expressing the average extractable power as a function of the maximum flow rate in the undisturbed regime, Q_0, produces a convenient result. In this analysis, the non-dimensional *relative* power is defined as

$$P_{rel}^{*} = \frac{P_{avg}^{*}}{Q_0^{*}} . \tag{2.38}$$

The maximum relative power is defined as the multiplier, γ, as

$$\gamma = \left(P_{rel}^{*} \right)_{\max} . \tag{2.39}$$

Garrett and Cummins [6] showed that the multiplier, γ, only varies between 0.25 and 0.19 for a channel connecting two large basins; the case defined in this analysis as $\beta = 0$.

The maximum average extractable power for electricity generation may then be defined as

$$\left(P_{avg}\right)_{\max} = \gamma \rho g a Q_0 , \tag{2.40}$$

where the multiplier, γ, is expected to only slightly vary for any channel linking a bay to the open ocean. This is convenient since the extractable power may be estimated if the maximum water surface elevation just outside the channel in the open ocean and the maximum flow rate in the undisturbed state are known.

2.4 Summary

The momentum balance for the flow through the channel may be defined as

$$\frac{dQ^*}{dt^*} = \zeta_0^* - \zeta_{Bay}^* - \lambda_1^* Q^* \left|Q^*\right|^{n_1-1} - \lambda_2^* Q^* \left|Q^*\right|^{n_2-1} - \frac{ga}{2(c\omega E_L)^2} Q^* \left|Q^*\right|. \tag{2.41}$$

where $Q^* = \frac{c\omega}{ga} Q$, $t^* = \omega t$, $\zeta_0^* = \frac{\zeta_0}{a}$, $\zeta_{Bay}^* = \frac{\zeta_{Bay}}{a}$, $\lambda_1^* = \lambda_1 \frac{(ga)^{n_1-1}}{(c\omega)^{n_1}}$, and $\lambda_2^* = \lambda_2 \frac{(ga)^{n_2-1}}{(c\omega)^{n_2}}$.

The dependence of the water surface elevation within the bay on the flow rate through the channel was derived from continuity to be

$$\frac{d\zeta_{Bay}^*}{dt^*} = \beta Q^*. \tag{2.42}$$

Solving equations (2.41) and (2.42) simultaneously, the average extractable power for electricity generation, as a function of the volume flow rate and turbine drag parameter is

$$P_{avg}^* = \lambda_1^* \overline{Q^{*2} \left|Q^*\right|^{n_1-1}}. \tag{2.43}$$

Chapter 3

Results and Discussion

Three scenarios are explored and compared below. The first two scenarios assume that bottom drag and exit flow separation within the channel are negligible. Two drag laws are explored. The first scenario assumes that the turbine drag is linearly proportional to the flow rate, whereas, the second scenario assumes that the turbine drag is quadratic in the flow rate. The third scenario includes bottom drag and exit flow separation in the momentum balance and assumes that bottom drag and turbine drag are quadratic in the flow rate. The average extractable power for electricity generation is calculated for all scenarios and comparisons are made.

The water surface elevation just outside the channel entrance in the open ocean is approximated by a single sinusoidal wave form with amplitude, a, and frequency, ω. Therefore,

$$\zeta_0 = a\cos\omega t, \tag{3.1}$$

which is expressed in its non-dimensional form as $\zeta_0^* = \cos t^*$.

3.1 Negligible Bottom Drag and Exit Separation Effects

Two drag laws are explored when bottom drag and exit separation effects are assumed negligible: linear and quadratic relationships with the volume flow rate. An analytic solution, presented in detail in Appendix A, for the model is obtained when turbine drag is assumed to be linearly proportional to the volume flow rate. When the drag is assumed to be quadratic, a numerical solver is developed to obtain a numerical solution since the coupled ordinary differential equations are non-linear. As stated in Csanady [18], the most realistic representation of bottom drag is quadratic with the flow rate. While the linear case may be less representative of the natural system, the analytic solution does provide insight into the underlying physics of the problem and provides validation for the numerical solver.

3.1.1 Linear Drag – Analytic Solution

When bottom drag and exit separation effects are assumed negligible and turbine drag is assumed to be linear, the momentum balance may be written as

$$\frac{dQ^*}{dt^*} = \cos t^* - \zeta_{Bay}^* - \lambda_1^* Q^* . \tag{3.2}$$

Equations (3.2) and (2.31) are solved simultaneously. The non-dimensional flow rate and water surface elevation within the bay are solved to be

$$Q^* = \frac{\lambda_1^* \cos t^* - (\beta - 1)\sin t^*}{(\beta - 1)^2 + \lambda_1^{*2}}, \tag{3.3}$$

and

$$\zeta_{Bay}^{*} = \frac{\beta(\beta-1)\cos t^{*} + \beta\lambda_1^{*}\sin t^{*}}{(\beta-1)^2 + \lambda_1^{*2}}, \tag{3.4}$$

respectively. The complex form of the non-dimensional water surface elevation within the bay is

$$\zeta_{Bay}^{*} = \frac{\beta}{(\beta-1)^2 + \lambda_1^{2}}\left[(\beta-1) - \lambda_1 i\right]. \tag{3.5}$$

The complex modulus and phase of the non-dimensional water surface elevation within the bay are

$$\left|\zeta_{Bay}^{*}\right| = \frac{\beta}{\left[(\beta-1)^2 + \lambda_1^{*2}\right]^{1/2}}, \tag{3.6}$$

and

$$\theta = \tan^{-1}\left(\frac{\lambda_1}{\beta-1}\right). \tag{3.7}$$

The value of θ is between 0° and 180°. The phase lag is plotted in Figure 3.1 as a function of the bay geometry term and the turbine drag parameter.

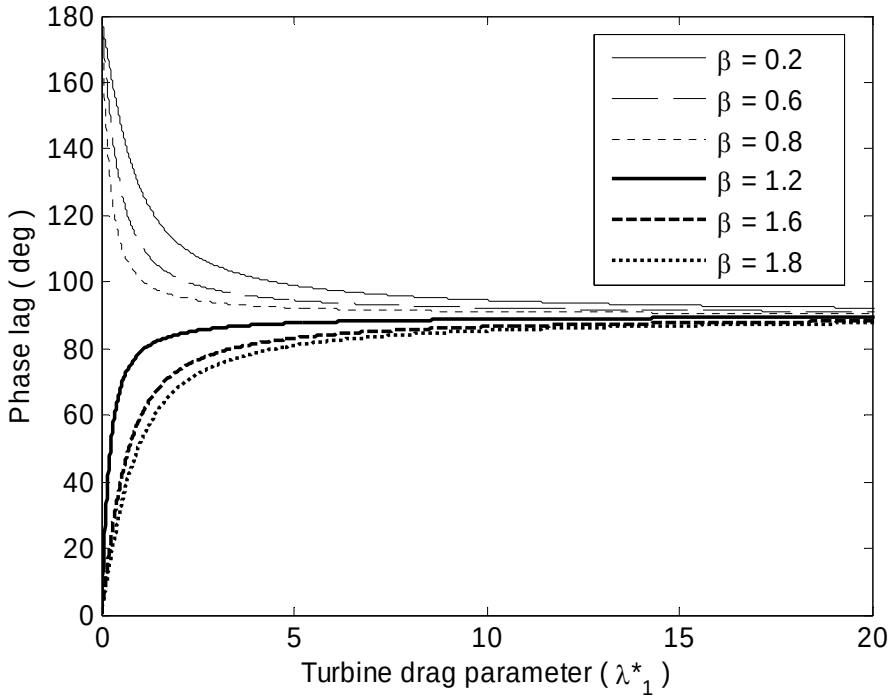

Figure 3.1: Phase lag as a function of the turbine drag parameter for varying bay geometries when drag is assumed to be linear with the volume flow rate.

The non-dimensional average extractable power is plotted in Figure 3.2, as function of the turbine drag parameter, for varying β. Since bottom drag and drag on support structures are assumed negligible, all of the extractable power from the channel is extracted for electricity generation. The maximum non-dimensional average extractable power grows exponentially as the bay geometry approaches the Helmholtz resonance corresponding to $\beta = 1$. Please refer to Appendix C for a full derivation of the Helmholtz frequency and further explanation.

The relative power, defined in equation (2.38), is plotted in Figure 3.3, as a function of the turbine drag parameter for varying bay geometries. The multiplier, γ, is equal

to 0.25 for all values of β. Therefore, when the turbine drag is linearly proportional to the volume flow rate and bottom drag and exit separation effects within the channel are negligible, the maximum average extractable power over the tidal cycle is

$$\left(P_{avg}\right)_{\max} = 0.25\rho g a Q_0 , \tag{3.8}$$

for all values of β. The multiplier, γ, will be shown in Section 3.2.1 to decrease as increasing levels of losses occur in the channel.

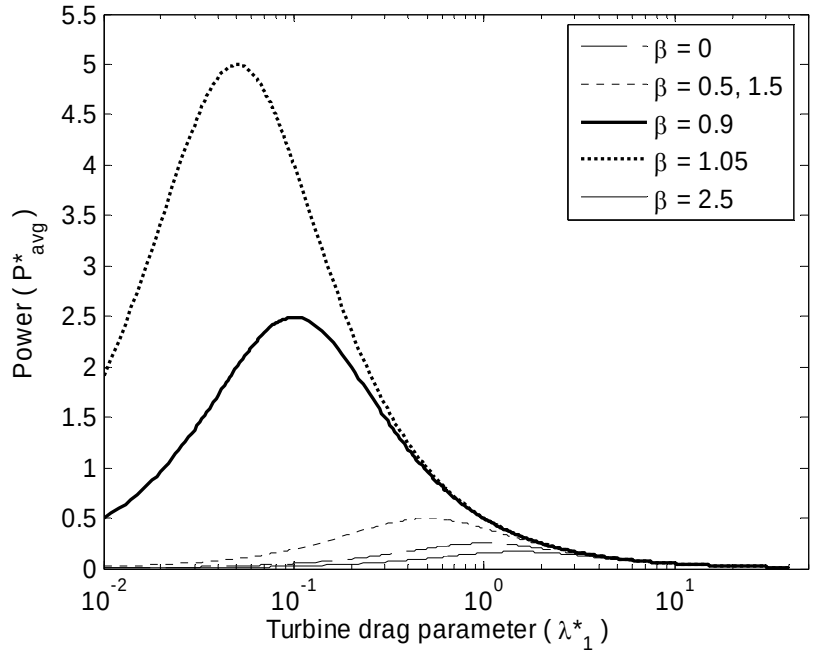

Figure 3.2: Non-dimensional average extractable power as a function of the turbine drag parameter for varying bay geometries when friction is assumed linearly proportional with the flow rate and losses are negligible.

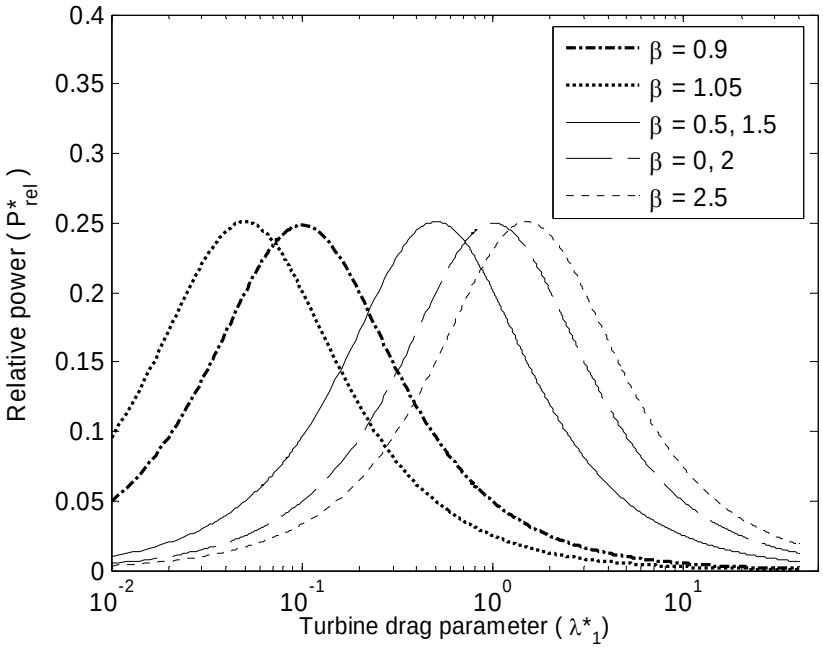

Figure 3.3: Relative power as a function of the turbine drag parameter for varying bay geometries when friction is assumed linearly proportional with the flow rate and losses are negligible.

3.1.2 Quadratic Drag – Numerical Solution

A numerical solver was developed in Matlab (The MathWorks Inc., Novi, MI) to calculate the average extractable power for the second scenario. Here, turbine drag is assumed to be quadratic in the volume flow rate. The program solves the non-dimensional, coupled, ordinary differential equations using the *ode45* Matlab function, returning volume flow rate and water surface elevation within the bay for varying values of β and drag within the channel. The *ode45* function, a one-step solver based on an explicit Runge-Kutta formula, integrates the system of differential equations over a prescribed time span based on an initial condition [19]. An adequate time span is essential for the solution to reach steady state. Once the solution converges, the program calculates the average power curves using equations (2.36) and (2.38). The program is able to solve both the linear and quadratic cases by allowing the exponent n_1 to vary arbitrarily. The numerical solver is validated based on the analytic solution by setting n_1 equal to unity.

The non-dimensional average extractable power for electricity generation, in this scenario, is

$$P_{avg}^{*} = \lambda_1^{*} \overline{Q^{*2} \left| Q^{*} \right|}. \tag{3.9}$$

The non-dimensional power curves for varying β and turbine drag parameter, λ_1^{*}, are plotted in Figure 3.4. The relative power curves are plotted in Figure 3.5. The

multiplier, γ, is only slightly different than in the linear case, varying between 0.25 and 0.24. Since bottom drag is assumed negligible, all the extractable power is for electricity generation.

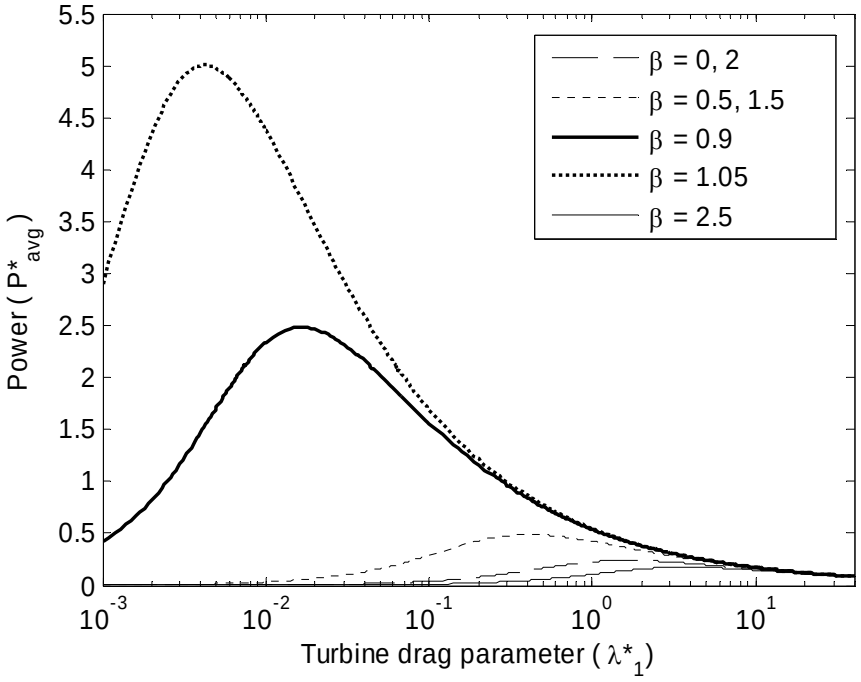

Figure 3.4: Non-dimensional average extractable power as a function of the turbine drag parameter for varying bay geometries when drag is assumed to be quadratic with the flow rate and losses are negligible.

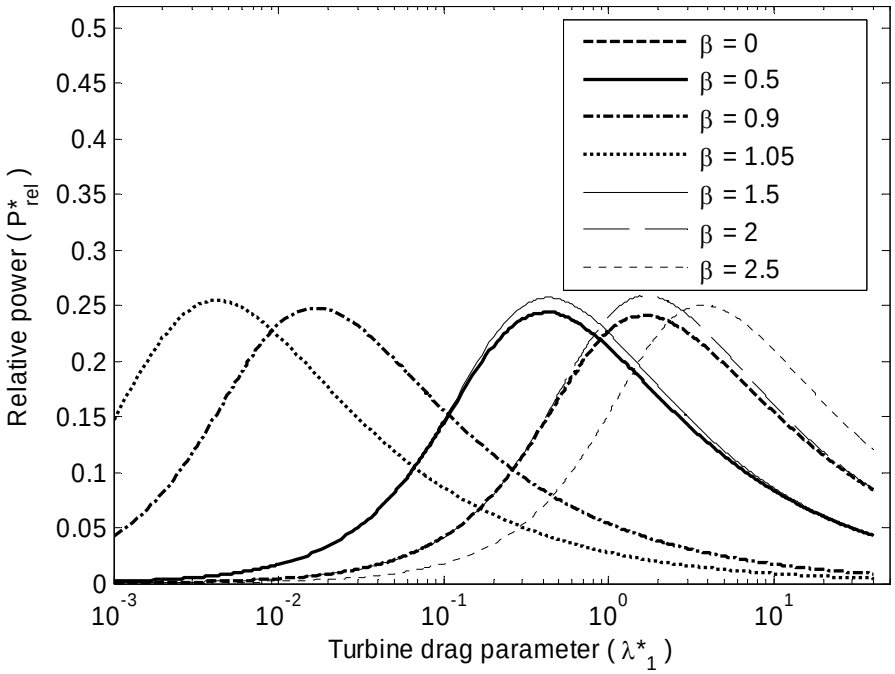

Figure 3.5: Relative power as a function of the turbine drag parameter for varying bay geometries when drag is assumed to be quadratic with the flow rate and losses are negligible.

3.1.3 Validation

The numerical solver may be validated based on the results provided by Garrett and Cummins [6] for a channel linking two large basins. This scenario is defined in the present analysis as $\beta = 0$. The two basins are large enough that they have their own tidal regimes, independent of the flow through the channel. Indeed, if the surface area of the bay is sufficiently large, $\beta \approx 0$. The non-dimensional average extractable power for both the linear and quadratic drag laws when $\beta = 0$ and bottom drag and exit separation effects are negligible, are plotted in Figure 3.6. The numerical solver does in fact provide the exact same solution as presented in Garrett and Cummins [6].

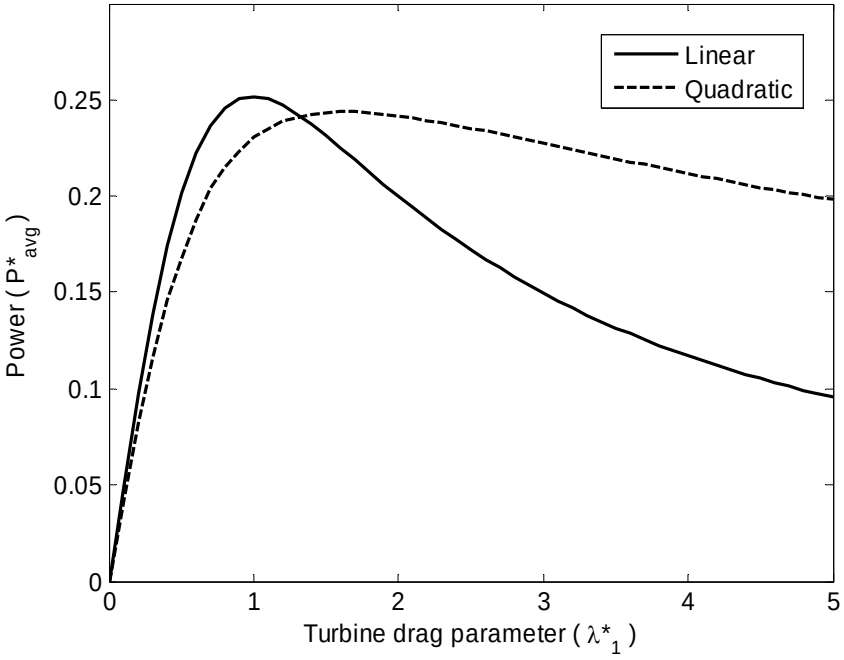

Figure 3.6: Non-dimensional average extractable power for linear and quadratic drag cases when $\beta = 0$ and losses are assumed negligible.

The maximum average extractable power for the linear case, when $\beta = 0$ is

$$\left(P_{avg}\right)_{\max} = \frac{1}{4}\rho\frac{(ga)^2}{c\omega} = 0.25\rho gaQ_0\,, \tag{3.10}$$

since $Q_0 = ga(\omega c)^{-1}$.

The maximum average extractable power is reduced to 97% of this value when quadratic friction is assumed, as shown in Figure 3.6. This result was also shown in Garrett and Cummins [6].

This validation simply provides confidence in the numerical solver and its ability to solve the coupled ordinary differential equation based on published results given in Garrett and Cummins [6].

3.2 Including Bottom Drag and Separation Effects - Quadratic Drag

Bottom drag and exit separation effects are now included in the momentum balance. Both bottom drag and turbine drag are assumed to be quadratic with the flow rate for the remainder of the analysis. Please refer to Appendix B for a detailed explanation for this case. In this scenario, the bottom drag and exit separation term may be grouped into one non-dimensional loss parameter, λ_0^*, where

$$\lambda_0^* = \frac{ag}{(c\omega)^2}\left[\int_0^L C_d (hE^2)^{-1} dx + (2E_L^2)^{-1}\right]. \tag{3.11}$$

The momentum balance may, therefore, be written as

$$\frac{dQ^*}{dt^*} = \cos t^* - \zeta_{Bay}^* - (\lambda_1^* + \lambda_0^*)\left|Q^*\right|Q^*. \tag{3.12}$$

3.2.1 Maximum Extractable Power

The maximum non-dimensional extractable power for electricity generation is plotted in Figure 3.7, and is shown to decrease for increasing λ_0^*. For channels dominated by bottom drag and exit separation effects, the average extractable poweris shown to converge to approximately $0.1\rho(ga)^2(c\omega)^{-1}$ for all β. The multiplier, γ, plotted in Figure 3.8, varies between approximately 0.26 and 0.19 and converges to approximately 0.21 for $\lambda_0^* \geq 3$. The maximum average extractable power for electricity generation may, therefore, be estimated to within approximately 10 - 15%, as $0.22\rho gaQ_0$ for all β without understanding the basic dynamic balance.

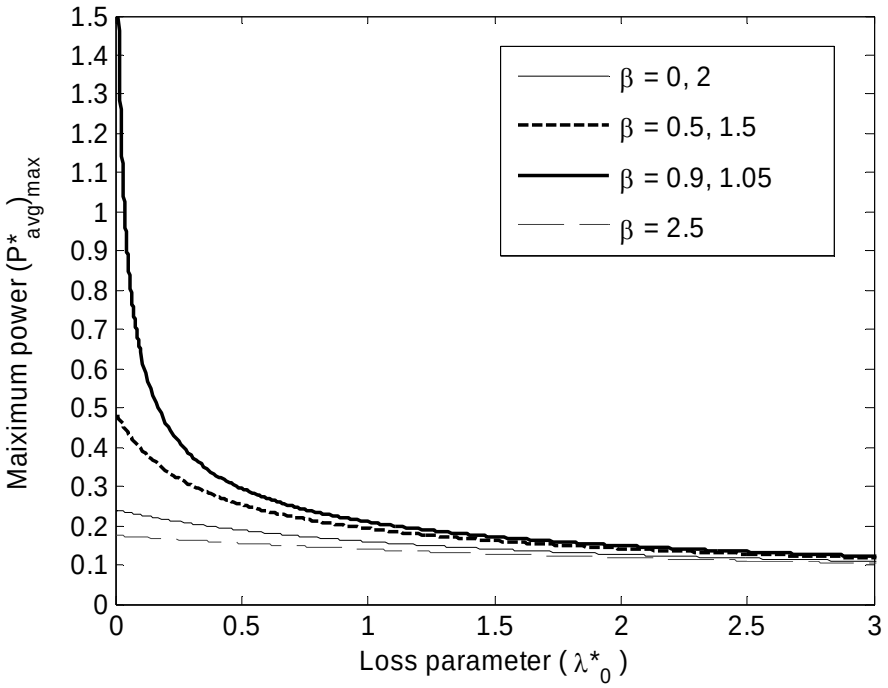

Figure 3.7: Maximum non-dimensional average extractable power as a function of the loss parameter for varying bay geometries when drag is assumed to be quadratic with the flow rate.

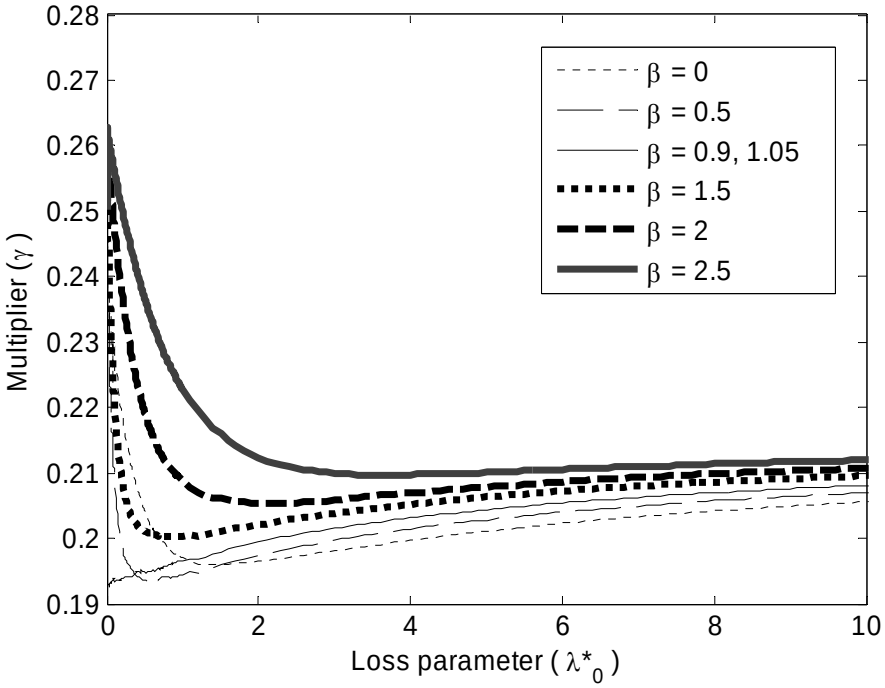

Figure 3.8: Multiplier as a function of the loss parameter for varying bay geometries when drag is assumed to be quadratic with the flow rate.

3.2.2 Validation

The numerical solution presented in Chapter 3.2.1 may be validated based on results published in Garrett and Cummins [6]. The maximum average extractable power for increasing λ_0^* for a channel connecting two large basins ($\beta = 0$) is plotted in Figure 3.9. The maximum average extractable power is approximately $0.24\rho(ga)^2(c\omega)^{-1}$ when bottom drag and exit separation effects are negligible and decreases to approximately $0.045\rho(ga)^2(c\omega)^{-1}$ for channels dominated by them. These results agree exactly with those determined presented in [6].

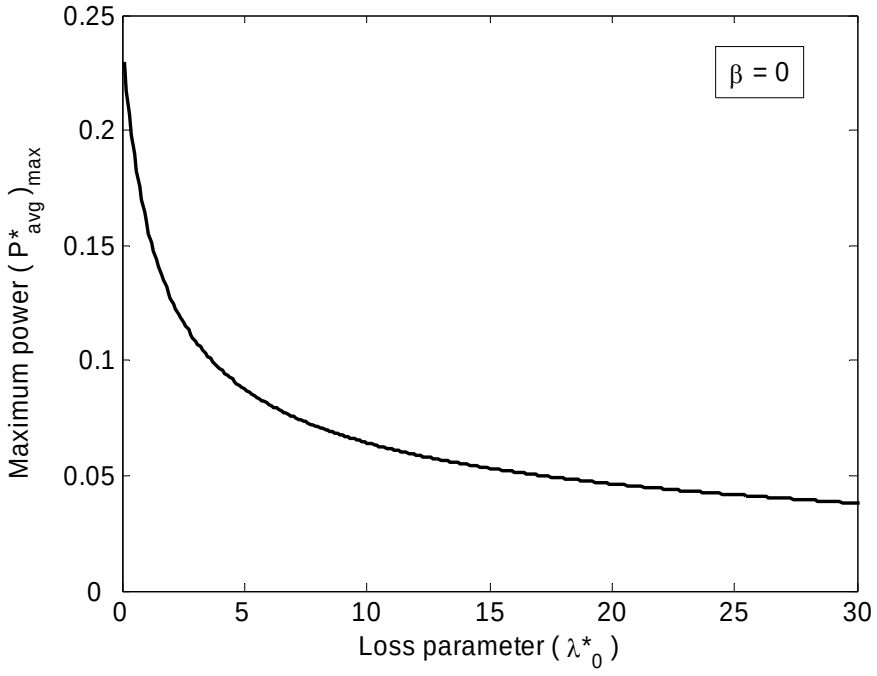

Figure 3.9: Maximum non-dimensional average extractable power for $\beta = 0$ as a function of the loss parameter.

This validation provides additional confidence in the numerical solver. Further validation is necessary, however, to verify how accurately the mathematical model predicts observable flows in tidal streams. This will be presented later, in Chapter 4, in the case study for Masset Sound, Haida Gwaii.

3.2.3 Determining Bay Geometry Term and Loss Parameter

Two methods are explored to calculate the bay geometry term, β, and the loss parameter, λ_0^*, for a channel connecting a bay to the open ocean. In the first method, the bay geometry term, β, defined in equation (2.30) as $g(cA\omega^2)^{-1}$ is calculated by measuring the surface area of the bay, A, and the channel geometry term, c. The loss parameter, λ_0^*, is then calculated using equation (3.11) and a typical drag coefficient for the region. In the second method, the modelling results are applied to determine the bay geometry term and loss parameter based on the observable amplitude ratio and phase lag of the tidal regime within the bay in the undisturbed regime.

The amplitude ratio is defined as

$$\left|\zeta_{Bay}^*\right| = \frac{\left|\zeta_{Bay}\right|}{a}. \tag{3.13}$$

The phase lag, defined in equation (3.7), is the lag of the maximum water surface elevation within the bay behind the maximum water surface elevation just outside the channel in the open ocean. The amplitude ratio and phase lag for varying β and λ_0^* are plotted in Figure 3.10 and Figure 3.11, respectively.

A contour plot of the amplitude ratio and phase lag was compiled using the data from Figure 3.10 and Figure 3.11, and plotted in Figure 3.12. The bay geometry term and

loss parameter for any bay may now be determined using Figure 3.12 if the amplitude and phase of the dominant tidal constituent at each end of the channel are known. For example, a bay with an amplitude ratio of 0.6 and a phase lag of 80° may be modelled as $\beta = 2$ and $\lambda_0^* = 12.5$.

The model predicts some additional interesting results. For instance, if $\beta < 2.5$ and the $\theta < 60^\circ$, the amplitude ratio is greater than one. The water surface elevation within the bay would, therefore, be larger than the water surface elevation just outside the channel in the open ocean. It is also apparent from Figure 3.12 that the model begins to break down as the loss parameter approaches zero and the bay geometry term approaches resonance. This was expected, as discussed in Appendix A, since it is physically impossible for a channel to have zero drag.

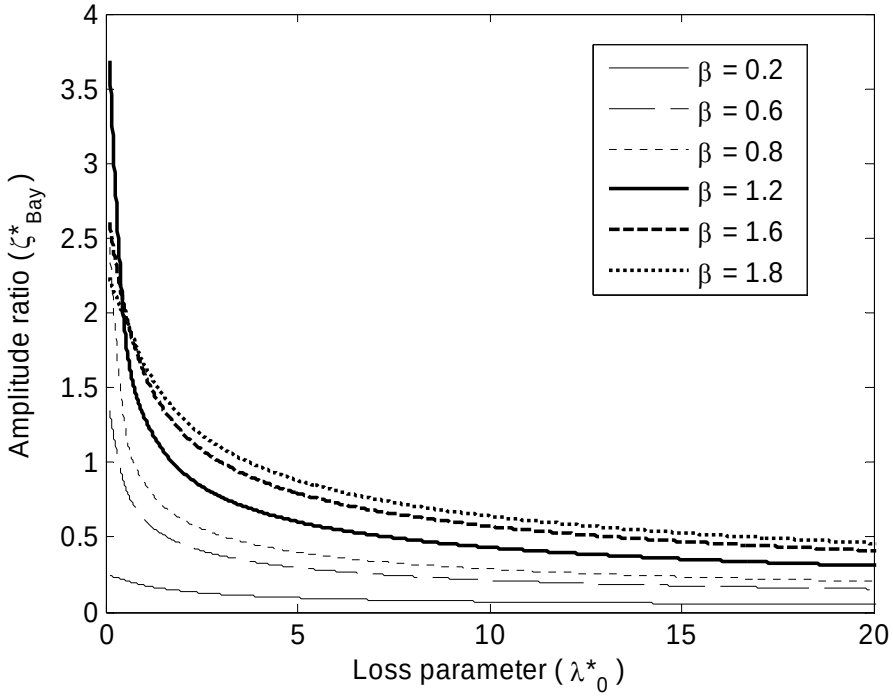

Figure 3.10: Amplitude ratio as a function of the loss parameter for varying bay geometries when drag is assumed to be quadratic with the flow rate

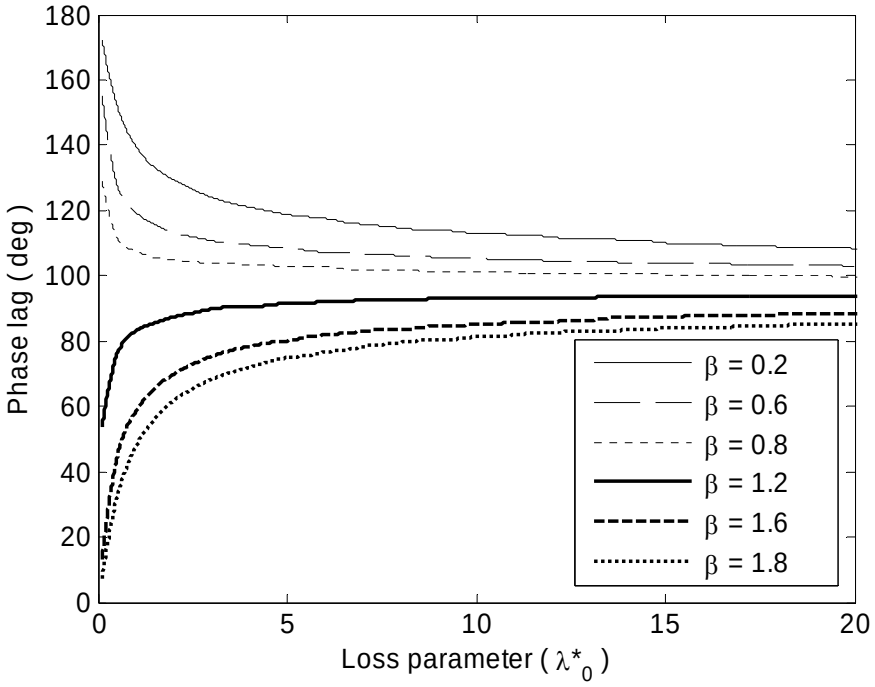

Figure 3.11: Phase lag as a function of the loss parameter for varying bay geometries when drag is assumed to be quadratic with the flow rate

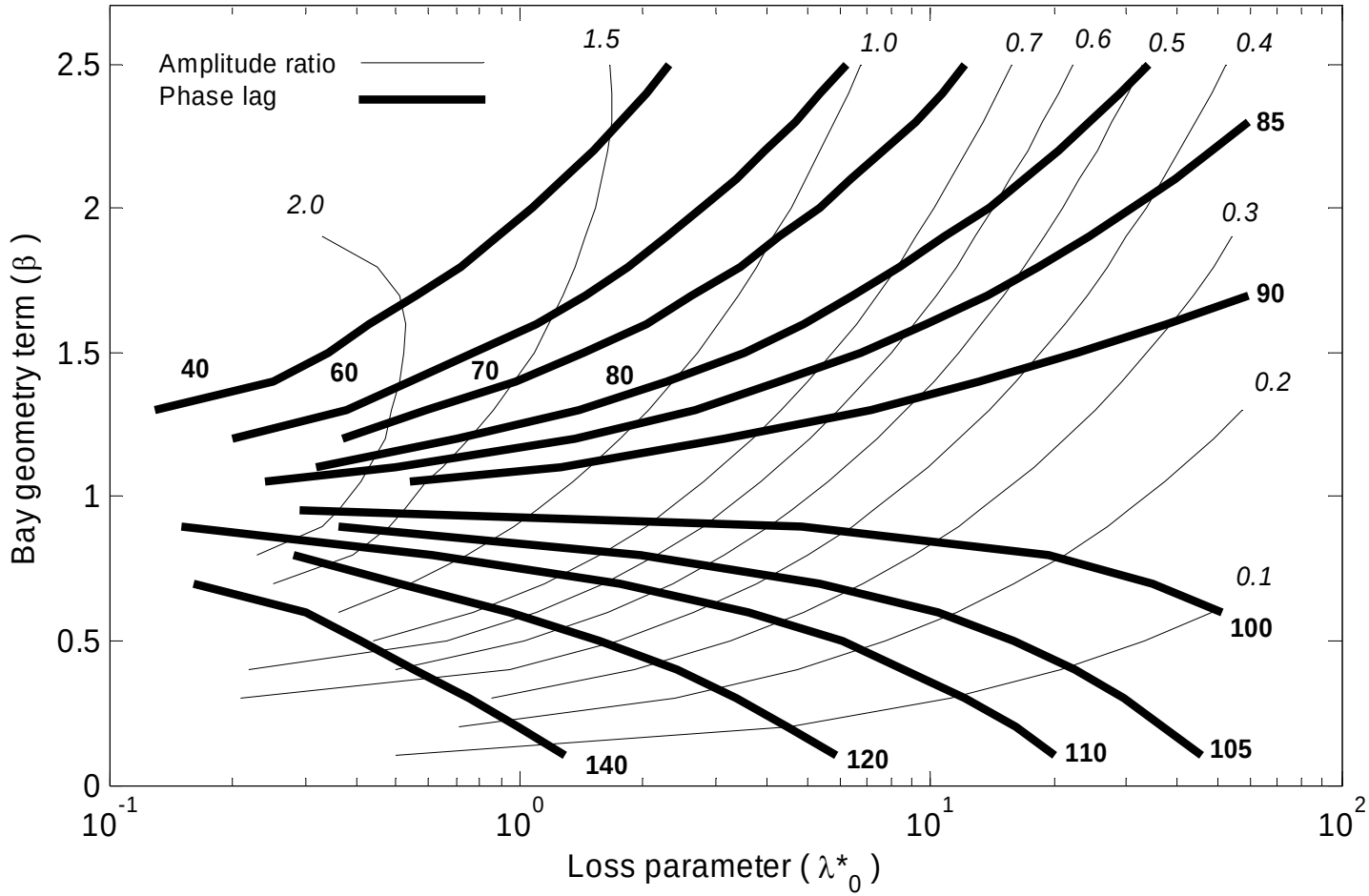

Figure 3.12: Light line represents various values of the amplitude ratio (in italic). Dark line represents various values of phase lag in degrees (in bold). Contours are a function of the loss parameter and the bay geometry term.

3.3 Summary

The tidal stream power model has now been developed to mathematically model the flow through a channel linking a bay to the open ocean. The most sophisticated scenario explored in this thesis assumes that drag has a quadratic dependence on the volume flow rate and includes bottom drag and exit separation effects in the momentum balance. The bay geometry term, β, and loss parameter, λ_0^*, for a channel linking a bay to the open ocean may be calculated using two different methods. In the first method, the bay geometry term is calculated based on measuring the surface area of the bay and the cross-sectional area of the channel over its entire length. The loss parameter is then calculated based on a typical drag coefficient for the region. In the second method, the contour plot presented in Figure 3.12 is used to determine the bay geometry term and loss parameter based on the amplitude ratio and phase lag in the undisturbed state.

Once β and λ_0^* are known, the average extractable power for a given bay may be calculated. A detailed case study is now presented for Masset Sound and Masset Inlet to validate the model and explore the potential for tidal stream power in a remote island region.

Chapter 4

Masset Sound Case Study

4.1 Introduction

The tidal stream power model was applied to Masset Sound and Masset Inlet in Haida Gwaii (Queen Charlotte Islands) to estimate the average extractable power for electricity generation. Haida Gwaii is a remote island region off the west coast of British Columbia, Canada. The total cost of generating electricity on Haida Gwaii ranges between 17 and 21 cents/kWh [20], whereas British Columbians are typically charged approximately 6.6 cents/kWh for their electricity [21]. The peak demand for Haida Gwaii is approximately 10 MW [22]. Masset Sound may be a suitable location for tidal stream power generation due to the high cost of fuel associated with the existing and predominantly diesel-fuelled power generation, strong tidal currents [23], and close proximity to major load centers and transmission lines.

4.2 Tidal Regime

The tidal regimes for Canadian coastlines have been closely analyzed by CHS. Tidal constituents for a local tidal regime are calculated from data obtained from water surface elevation data. The amplitude, a, and phase angle, ϕ, of all tidal constituents are available from CHS [11]. The tidal constituents for Wiah Point and Port Clements (Figure 4.1) will be used to model the water surface elevations of the open ocean and the bay, respectively. Tidal predictions for both these locations, over a seven day period, beginning January 7, 2007 are shown in Figure 4.2 [11].

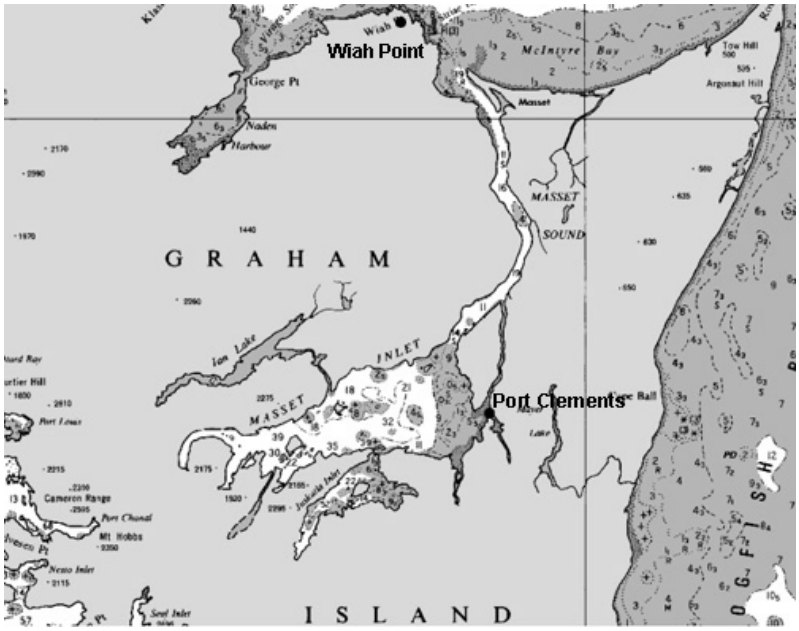

Figure 4.1: Masset Sound on Graham Island in Haida Gwaii [24].

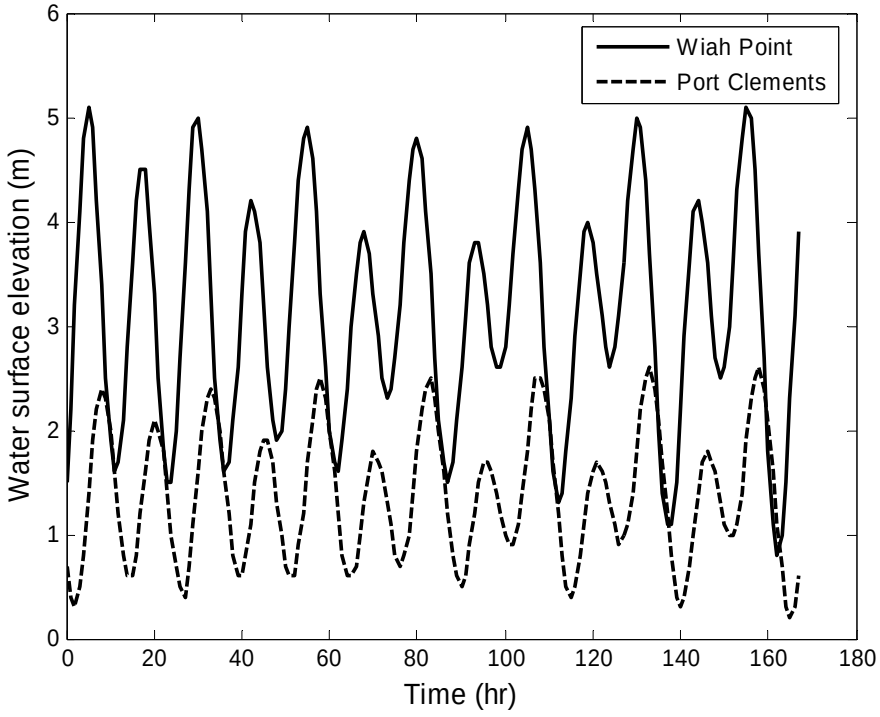

Figure 4.2: CHS tidal predictions for Wiah Point and Port Clements [11].

Presently, the model assumes that the tidal regime may be expressed as a single sinusoidal waveform. It is apparent from Figure 4.2, however, that the tidal regime in Masset Sound is composed of multiple tidal constituents. The dominant tidal constituent for Wiah Point and Port Clements is the semi-diurnal (twice daily) M2 tide with a frequency of $1.4\times10^{-4}\,\mathrm{s}^{-1}$ and amplitudes of 1.47 m and 0.80 m, respectively. A single sinusoid of the form,

$$\zeta_0 = a\cos\omega t\,, \tag{4.1}$$

is, therefore, assumed to accurately describe the tidal regime at Wiah Point where a = 1.47 m and $\omega = 1.4\times10^{-4}\,\mathrm{s}^{-1}$.

The volume flow rate, Q, and water surface elevation within the bay, ζ_{Bay}, were shown in equations (3.12) and (2.31) to be a function of the bay geometry term, β, and the non-dimensional loss parameter, λ_0^*. Therefore, β and λ_0^* must be determined to assess the tidal stream power resource.

4.3 Determining the Bay Geometry Term and Loss Parameter

4.3.1 Method #1 – Bathymetric Data and Amplitude Ratio

The bay geometry term is a function of the surface area of the bay and the channel geometry term as presented in equation (2.30). The surface areas of Masset Inlet (Figure 4.3) and Masset Sound (Figure 4.4) were measured to be approximately 238 km^2 and 49 km^2, respectively, using the Land and Resource Data Warehouse

Catalogue [25] available from the Government of British Columbia. The channel geometry term, *c*, for Masset Sound was calculated by digitizing the highest resolution chart soundings available from CHS using ArcGis-ArcInfo version 9.1 (ESRI, US). The digitized soundings were interpolated into a 40 m by 40 m grid using a spline interpolation. The digitized channel is shown in Figure 4.5. The channel geometry term was calculated as $1.64\ \mathrm{m}^{-1}$. Substituting $g = 9.81\ \mathrm{ms}^{-2}$, $c = 1.64\ \mathrm{m}^{-1}$, $A = 238\ \mathrm{km}^2$, and $\omega = 1.4\times10^{-4}\ \mathrm{s}^{-1}$ into equation (2.30), the bay geometry term for Masset Sound is

$$\beta = 1.28\,. \tag{4.2}$$

An average water depth of 14 m and an average cross-sectional area of $1.7\times10^{4}\ \mathrm{m}^2$ are used for the values of *h* and *E*, respectively. The average cross-sectional area at either end of the channel is approximately $1.5\times10^{4}\ \mathrm{m}^2$ and the channel is approximately 27 km long. The typical bottom drag coefficient, C_d, for the region is 3.0×10^{-3} [10]. Substituting these values into equation (3.11), the loss parameter is

$$\lambda_0^* = 6\,. \tag{4.3}$$

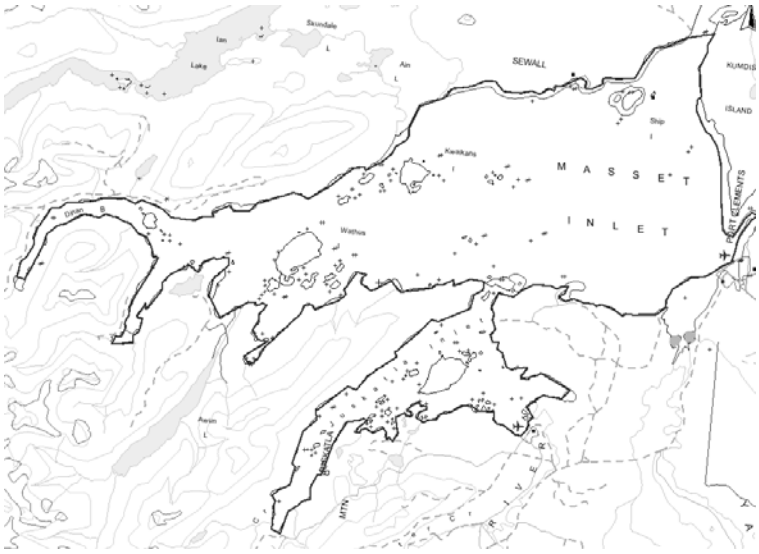

Figure 4.3: Masset Inlet [25].

Figure 4.4: Masset Sound [25].

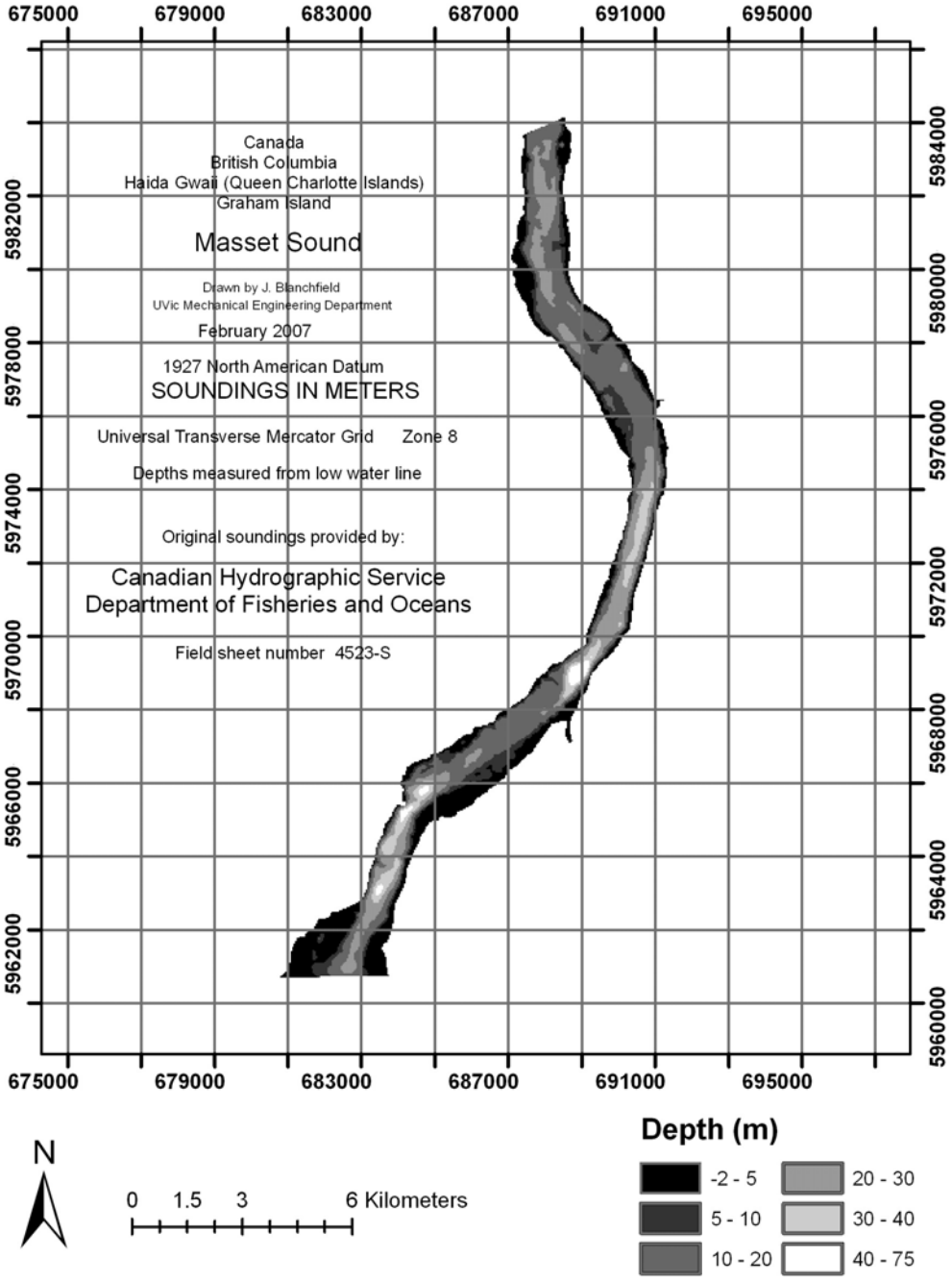

Figure 4.5: Digitized soundings for Masset Sound.

4.3.2 Method #2 – Amplitude Ratio and Phase Lag

The modelling results presented in Chapter 3.2 may also be used to calculate the bay geometry term and loss parameter based on the observed amplitude ratio and phase lag in the undisturbed state. The maximum water surface elevation within the bay, $\left|\zeta_{Bay}\right|$, is 0.80 m. The amplitude ratio is, therefore,

$$\frac{\left|\zeta_{Bay}\right|}{a} = 0.54 . \tag{4.4}$$

The phase angles of the M2 tides at Wiah Point and Port Clements are 33° and 121°, respectively. Therefore, the maximum water surface elevation within the bay lags the maximum water surface elevation in the open ocean just outside the channel by θ = 88°.

Based on the contour plot presented in Figure 3.12, a channel linking a bay to the open ocean with an observed phase lag of 88° and an amplitude ratio of 0.54 is associated with $\beta = 1.45$ and $\lambda_0^* = 8$.

Rearranging equation (2.30), the channel geometry term is

$$c = \frac{g}{\beta A \omega^2} . \tag{4.5}$$

The model, therefore, predicts a channel geometry term of 1.45 m^{-1}. This is 13% less than the channel geometry term that was calculated using bathymetric data in the first method.

Rearranging equation (3.11), the bottom drag coefficient is

$$C_d = \left[\lambda_0^* \frac{(c\omega)^2}{ga} - \frac{1}{2E_L^2} \right] \left(\frac{L}{hE^2} \right)^{-1}. \qquad (4.6)$$

It is apparent from equation (4.6) that the drag coefficient is sensitive to the loss parameter and the exit cross-sectional area. If we assume that $E_L = 1.5\times10^4\,m^2$, the first term inside the square bracket in equation (4.6) is $2.3\times10^{-8}\,m^{-4}$ and the second term is $2.2\times10^{-9}\,m^{-4}$, a factor of 10 smaller than the first term. This implies that the estimated drag coefficient is not particularly sensitive to the cross-sectional area where the flow is exiting to Masset Inlet or the Pacific ocean.

If we assume once more that h = 14 m, $E = 1.7\times10^4\,m^2$, L = 27 km, the model predicts a bottom drag coefficient of 3.1×10^{-3}, close to the regions typical drag coefficient.

The maximum non-dimensional volume flow rate for a bay defined by $\beta = 1.45$ is plotted as a function of the loss parameter in Figure 4.6. The maximum non-

dimensional volume flow rate in Masset Sound, with a loss parameter of $\lambda_0^* = 8$, is 0.35. Since

$$Q = \frac{ga}{c\omega} Q^*, \tag{4.7}$$

the maximum volume flow rate, Q_0, is approximately $2.5 \times 10^4\ \mathrm{m^3 s^{-1}}$.

It was shown in the analytic solution (Appendix A) that

$$Q = \omega A \left| \zeta_{Bay} \right|, \tag{4.8}$$

when drag is assumed linear in the flow rate. For Masset Sound, this corresponds to a maximum volume flow rate of $2.7 \times 10^4\ \mathrm{m^3 s^{-1}}$, only 8% greater than the results based on the quadratic drag assumption.

The smallest cross-sectional area, $E_{\min}$, in Masset Sound is approximately $1.0 \times 10^4\ \mathrm{m^2}$ located near UTM northing 5975500 (see Figure 4.5). Since

$$u = \frac{Q}{E}, \tag{4.9}$$

where u is the flow velocity, the maximum flow velocity, u_{max}, in Masset Sound is estimated to be 2.5 ms^{-1} which agrees with the observed maximum flow speeds in the area [**22**].

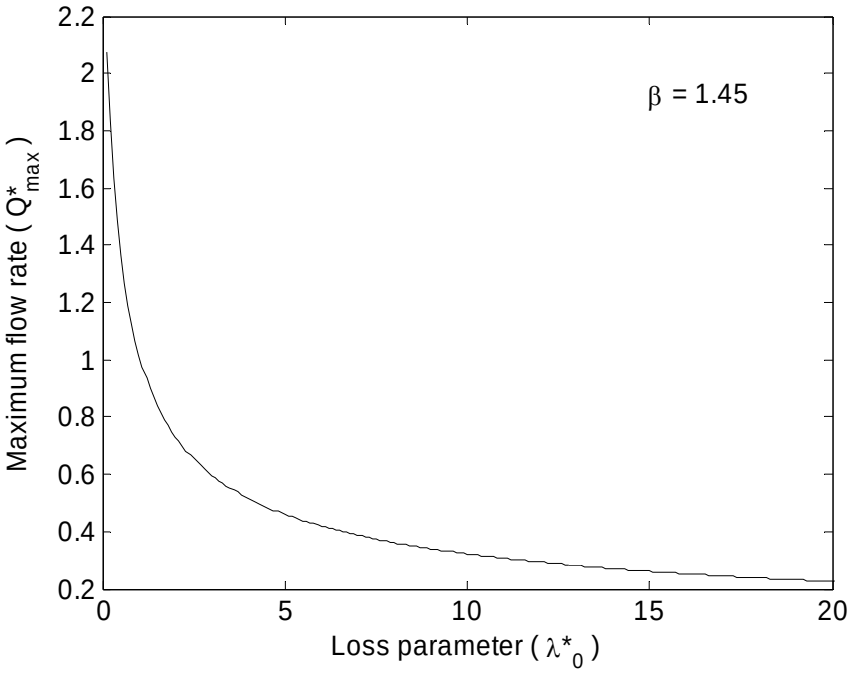

Figure 4.6: Maximum non-dimensional flow rate as a function of the loss parameter for a bay defined by β = 1.45.

4.5 Extractable Power

Initially, the average extractable power for electricity generation increases as turbines are installed in the tidal stream. Too many turbines, however, will excessively reduce the volume flow rate and eventually reduce the extractable power. The non-dimensional average extractable power is plotted in Figure 4.7 as a function of the turbine drag parameter, λ_1^*, for $\beta = 1.45$ and $\lambda_0^* = 8$. A maximum of $P_{avg}^* = 7.5 \times 10^{-2}$

is calculated when $\lambda_1^* = 15$. Substituting equation (4.5) into equation (2.37), the average extractable power may be written as

$$P_{avg} = P_{avg}^* \beta \rho g a^2 A \omega . \tag{4.10}$$

Substituting $P_{avg}^* = 7.5 \times 10^{-2}$ into equation (4.10), the maximum average extractable power is 79 MW.

The power multiplier, γ, is plotted in Figure 4.8 as a function of the loss parameter for β = 1.45. The maximum average extractable power from Masset Sound is approximately equal to

$$\left(P_{rel}\right)_{\max} = 0.21 \rho g a Q_0 . \tag{4.11}$$

It may be impractical to exploit the maximum average extractable power due to the perturbations to the tidal regime associated with extracting the maximum extractable power. The perturbations to the water surface elevation within the bay and the volume flow rate through the channel are now analyzed for different levels of power extraction.

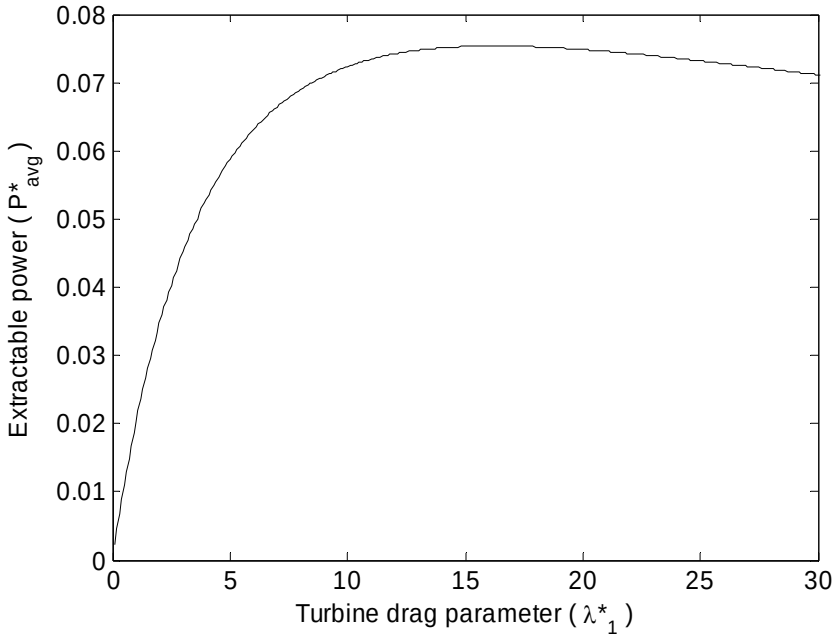

Figure 4.7: Non-dimensional average extractable power as a function of the turbine drag parameter for Masset Sound when defined by $\beta = 1.45$ and $\lambda_0^* = 8$.

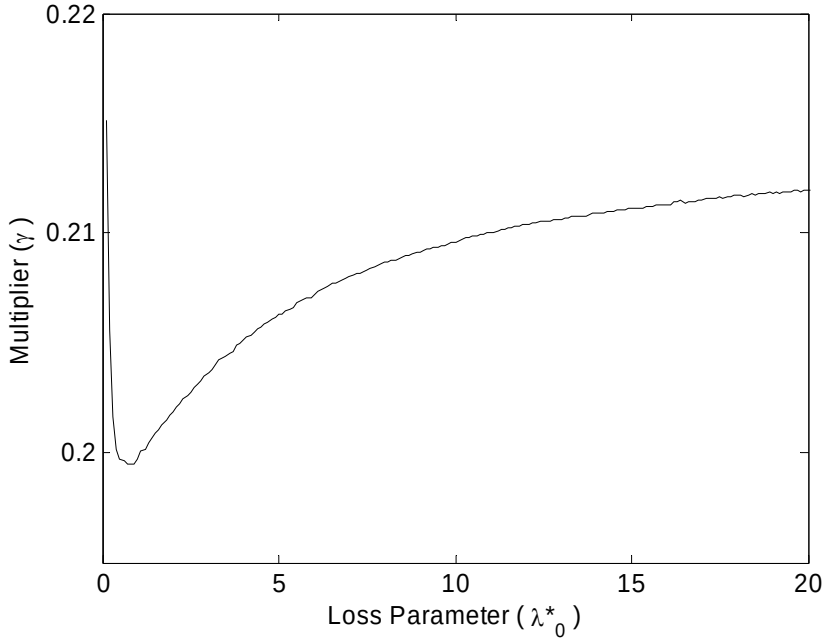

Figure 4.8: Power multiplier as a function of the loss parameter for Masset Sound as defined by $\beta = 1.45$.

4.6 Tidal Regime Perturbation

The water surface elevation within the bay and the volume flow rate through the channel decrease as power is extracted from Masset Sound for electricity generation. For this analysis, perturbations to the tide regime are explored when Masset Sound is defined by $\beta = 1.45$, $\lambda_0^* = 8$, and the tides at Wiah Point are approximated as a single sinusoid.

When 79 MW is extracted, the water surface elevation within the bay and maximum volume flow rate are reduced to 58% of the undisturbed state. The tidal regime may be kept to within 90% of the undisturbed regime, while extracting 37 MW, when $\lambda_1^* = 2$. It is important to note, however, that the extractable power for electricity generation neglects mechanical and electrical inefficiencies of the turbines, and additional drag on the supporting structures; only a portion of this extractable power will be available to meet the load.

With a maximum load of approximately 10 MW, a significant amount of Haida Gwaii's electricity demand may be met using tidal energy extracted from Masset Sound, while maintaining 90% of the undisturbed tidal regime.

Chapter 5

Conclusions and Recommendations

This chapter summarizes the key objectives and major findings of this thesis. Recommendations for future work will be listed to aid in the continued development of this theory. The objectives of this thesis were to:

- develop a one-dimensional mathematical model describing the flow through a channel linking a bay to the open ocean, including flow acceleration, bottom drag and exit separation effects;

- determine the average extractable power of Masset Sound in Haida Gwaii, and quantify the associated perturbations to the tidal regime.

5.1 Conclusions

This thesis developed a one-dimensional mathematical model describing the average extractable power in a channel linking a bay to the open ocean. The dynamical balance includes flow acceleration, turbine drag, bottom drag, and exit separation effects. A numerical solver was developed to determine the volume flow rate through the channel, the water surface elevation within the bay, and the extractable power for various bay geometries.

The general conclusion is that the maximum average extractable power from a channel linking a bay to the open ocean may be estimated within approximately 10 -

15% as $0.22\rho gaQ_0$. The approximation assumes quadratic drag and a single sinusoidal forcing.

A contour plot has been developed to determine the bay geometry term and loss parameter for a bay, when the water surface elevation and phase of the tidal constituents at each end of the channel are known. This method is valuable since it eliminates the time and expense involved in obtaining the geometric values required to calculate the bay geometry term. The contour plot is only applicable for a channel linking a bay to the open ocean since it is a function of the amplitude ratio which is equal to zero for a channel linking two large basins. A detailed analysis for a bay linking two large basins, however, is presented in Garrett and Cummins [6].

A case study for Haida Gwaii reveals that the maximum average extractable power from Masset Sound is approximately 79 MW. It was determined that extracting 79 MW from Masset Sound would decrease the water surface elevation within the bay and the maximum volume flow rate through the channel by approximately 42% of its undisturbed regime. The tidal regime may be kept to within 90% of the undisturbed regime by limiting the average extracted power to 37 MW. Due to the low demand for electricity in the area, tidal energy may be able to provide Haida Gwaii with a significant amount of their electricity.

The bottom drag coefficient for Masset Sound was calculated to be 3.1×10^{-3}, which is approximately equal to the regions' typical drag coefficient presented in [10]. The

case study validated the mathematical model in predicting the undisturbed tidal regime of Masset Sound.

5.2 Recommendations

The following are recommendations for further research and additional projects that extend from this thesis:

- Modelling results within this thesis are based on the assumption that the tidal regime just outside the channel in the open ocean may be approximated by a single sinusoidal waveform. It would be valuable to explore the effects of describing the tidal regime with multiple tidal constituents. Garrett and Cummins [6] concluded that multiple constituents can be included in the analysis, where $\zeta_0 = a\cos\omega t + a_1\cos\omega_1 t + a_2\cos\omega_2 t + \ldots.$, but doing so depends on the basic dynamical balance. The extractable power calculated when $\zeta_0 = a\cos\omega t$ is multiplied by a factor of $1+(9/16)\left(r_1^2 + r_2^2 + \ldots\right)$, in the quasi-steady limit, where $r_1 = a_1/a$, $r_2 = a_2/a$ …, if the basic state is frictional, and $1+\left(r_1^2 + r_2^2 + \ldots\right)$ if the basic state is frictionless [6]. A similar analysis would be beneficial for all values of the bay geometry factor;

- Results have been based on increasing levels of the turbine drag parameter. It is essential that this term be related to the number of installed turbines, including the drag on the supporting structures;

- A case study exploring the integration of tidal stream power into the Haida Gwaii energy system based on a time series power generation would be very beneficial. It has been shown that increasing the turbine drag within Masset Sound will affect amount of extractable power and when it is available. There is an opportunity to optimize the installed capacity to meet the region's load.

References

[1] Triton Consultants Ltd. Green energy Study for British Columbia, Phase 2: Mainland, Tidal Current Energy 2002; Report prepared for BC Hydro.

[2] Triton Consultants Ltd. Canada Ocean Energy Atlas (Phase 1) Potential Tidal Current Energy Resources Analysis Background. Prepared for the Canadian Hyrdaulics Centre, May 2006.

[3] Black & Veatch Consulting. UK, Europe and Global Tidal Stream Energy Resource Assessment. Commissioned by the Carbon Trust 2004.

[4] Hagerman B, and Polagye. Guidelines for Preliminary Estimation of Power Production by Tidal In Stream (Current) Energy Conversion Devices, EPRI Guideline, EPRI– TP – 001 NA, 2005.

[5] Garrett C, and Cummins P. Generating power from tidal currents. Journal of Waterway, Port, Coastal and Ocean Engineering 2004; 130:114-118.

[6] Garrett C, and Cummins P. The power potential of tidal currents in channels. Proceedings of the Royal Society 2005; 461:2563-2572.

[7] Bryden IG, and Couch SG. ME1-marine energy extraction: tidal resource analysis. Renew. Energy 2006; 31:133-139.

[8] Bryden IG, and Melville GT. Choosing and Evaluating Sites for Tidal Current Development. Proc. Instn Mech. Engrs. 2004; Vol.218 Part A: J. Power and Energy.

[9] Thurman HV. Introductory Oceanography, 4th edition. Columbus, OH: Charles E. Merrill, 1985.

[10] Foreman MGG, Sutherland G, and Cummins P. M2 Tidal Dissipation around Vancouver Island: an Inverse Approach. Institute of Ocean Sciences, Department of Fisheries and Oceans, Continental Shelf Research, 2004; 24:2167-2185.

[11] Tides, Currents, and Water Levels, Canadian Hydrographic Service, Fisheries and Oceans Canada. [Online resource – cited May 2007]. Available http: www.waterlevels.gc.ca.

[12] Betz A. Das maximum der theoretisch moglichen ausutzung des wines durch windmotoren. Zeitschrift fur das gesamte turbinenwesen, 1920; Heft 26.

[13] Betz A.. Wind-Energie und ihre Ausnutzung durch Windmuhlen. Vandenhoek and Ruprecht, Gorringen 1926; pp 64.

[14] Lanchester FW. A contribution to the theory of propulsion and the screw propeller. Transanctions of the Institution of Naval Architects LVII. 1915; 98-116.

[15] Binnie and partners, Tidal Stream Energy Review, Energy Technology Support Unit (ETSU), DTI, T/05/00155 REP, 1993.

[16] The Exploitation of Tidal and Marine Currents, Commission of European Communities, Program Joule II, EUR 16683 ENm No, Jou2-CT93-0355, 1996.

[17] Scottish Enterprise, The Development and Market Potential for Tidal Current Power in Scotland, Robert Gorden University, Centre for Environmental Engineering and Sustainable Development, 2002

[18] Csanady GT. Circulation in the Coastal Ocean. Holland: D. Reidel Publishing Company, Dordrecht, 1982.

[19] Dormand JR, and Prince PJ. A family of embedded Runge-Kutta formulae, J. Comp. Appl. Math., 1980; 6:19-26.

[20] BC Hydro and Power Authority, Non-integrated Business Strategy, 2004.

[21] BC Hydro, Electricity Rates, [Online resource – cited March 2007]. Available http: http://www.bchydro.com/policies/rates/rates757.html.

[22] BC Hydro and Power Authority, Non-Integrated Business Strategy, January 8th, 2004.

[23] Canadian Tide and Current Tables. Queen Charlotte Sound to Dixon Entrance, Volume 7, Department of Fisheries and Oceans, Ottawa, Ontario, Canada, 2006.

[24] Digital Charts – Vancouver Island West – Queen Charlotte Islands, Canadian Hydrographic Service, Fisheries and Oceans Canada, 2007.

[25] Land and Resource Warehouse, Integrated Land Management Bureau, [Online resource – cited May 2007]. Available http: http://www.lrdw.ca/

[26] Thomson and Dahleh. Theory of Vibrations with Applications, 5th ed. Prentice Hall, New Jersey, 1998.

[27] Gorban AN, Gorlov AM, and Silantyex VM. Limits of the turbine efficiency for free fluid flow. *J. Energy Resour. Technol.* 2001; 123:311-317.

[28] Bryden IG, and Couch. The Impact of Energy Extraction on Tidal Flow Development. Centre for Research in Energy and the Environment, The Robert Gordon University, Scotland.

[29] Hammons TJ. Tidal power. Proceedings of the IEE. 1993; Vol8. No.3.

[30] Brooks D. The tidal-stream energy resource of Passamaquoddy-Cobscook Bays: A fresh look at an old story. Renewable Energy 31 2284 – 2295. 2006

[31] Queen Charlotte Islands Tidal Power Study. Prepared by BC Hydro and Nova Energy Ltd. 1984.

[32] Kowalik Z. Tide Distribution and Tapping into Tidal Energy. Institute of Oceanology PAS 2004; 291-331

.

Appendices

Appendix A – Negligible Bottom Drag and Exit Separation Effects - Linear Drag

An analytic solution is obtained when bottom drag and exit separation effects are assumed negligible, and turbine drag is assumed to be linearly proportional with the flow rate ($n_1 = 1$). Furthermore, the water surface elevation just outside the bay entrance in the open ocean is assumed to be a single sinusoidal waveform as

$$\zeta_0 = a \cos \omega t \,. \tag{A.1}$$

The non-dimensional water surface elevation is then

$$\zeta_0^* = \cos t^* \,. \tag{A.2}$$

Based on these assumptions, the momentum balance may then be written as

$$\frac{dQ^*}{dt^*} = \cos t^* - \zeta_{Bay}^* - \lambda_1^* Q^* \,. \tag{A.3}$$

From continuity,

$$\frac{d\zeta_{Bay}^{*}}{dt} = \beta Q^{*}. \tag{A.4}$$

Solving equations (A.3) and (A.4) simultaneously, the non-dimensional flow rate and water surface elevation within the bay are

$$Q^{*} = \frac{\lambda_1^{*}\cos t^{*} - (\beta - 1)\sin t^{*}}{(\beta - 1)^2 + \lambda_1^{*2}}, \tag{A.5}$$

and

$$\zeta_{Bay}^{*} = \frac{\beta(\beta - 1)\cos t^{*} + \beta\lambda_1^{*}\sin t^{*}}{(\beta - 1)^2 + \lambda_1^{*2}}, \tag{A.6}$$

respectively.

The non-dimensional average extractable power is

$$P_{avg}^{*} = \lambda_1^{*}\overline{Q^{*2}}. \tag{A.7}$$

Substituting (A.5) into (A.7), the average extractable power is

$$P_{avg}^{*} = \frac{1}{2}\frac{\lambda_1^{*}}{\left(\beta - 1\right)^2 + \lambda_1^{*2}}, \tag{A.8}$$

which is maximized when $\lambda_1^{*} = \beta - 1$ to be

$$\left(P_{avg}^{*}\right)_{\max} = \frac{1}{4}\frac{1}{\left(\beta - 1\right)}. \tag{A.9}$$

It is convenient to express the average extractable power as a function of the maximum flow rate in the undisturbed regime. The magnitude of the flow rate is maximized when $\lambda_1^{*} = 0$, to be

$$Q_0^{*} = \frac{1}{\left(\beta - 1\right)}. \tag{A.10}$$

The maximum flow rate in the undisturbed state may be expressed in its dimensional form as

$$Q_0 = \omega A\left|\zeta_{Bay}\right|. \tag{A.11}$$

A singularity exists in (A.10) when $\beta = 1$ since it assumed that there is no friction within the channel, which is physically impossible. This singularity may be avoided

by simply assigning a value of bottom drag parameter which is much less than the turbine drag parameter in order to maintain a negligible effect on the solution.

The relative power, defined as the non-dimensional average extracted power divided by the maximum non-dimensional flow rate in the undisturbed regime is

$$P_{rel}^{*} = \frac{1}{2}\frac{\lambda_1^{*}\left(\beta-1\right)}{\left(\beta-1\right)^2+\lambda_1^{*2}}. \tag{A.12}$$

The multiplier, γ, which is the maximum relative power, is 0.25 when $\lambda_1^{*} = \beta - 1$. Therefore, when friction is assumed to be linear and losses within the channel are assumed negligible, the maximum average extracted power for electricity generation is

$$\left(P_{avg}\right)_{\max} = 0.25\rho g a Q_0 . \tag{A.13}$$

Appendix B – Including Bottom Drag and Exit Separation Effects - Quadratic Drag

A more sophisticated and realistic model includes bottom drag and exit separation effects in the analysis. A numerical solution is required to solve for the non-dimensional flow rate and water surface elevation within the bay. For engineering applications, bottom drag is commonly assumed to be quadratic in the volume flow rate [18]. If drag is assumed to be quadratic $(n_1 = n_2 = 2)$, the bottom drag and the exit separation effect can be lumped together into the single term, λ_0, where

$$\lambda_0 = \lambda_2 + \frac{1}{2E_L^2}. \tag{B.1}$$

Assuming symmetry between the ebb and flood tides, the rise and fall of the tides are assumed to have a negligible effect on the exit area of the channel. Therefore, the loss parameter, $\lambda_0(E_L, t)$ is assumed to be constant throughout the tidal cycle.

Since the tidal regime in the open ocean is assumed to be a single sinusoidal wave form, the governing equation may be written as

$$\frac{dQ^*}{dt^*} = \cos t^* - \zeta_{Bay}^* - \left(\lambda_0^* + \lambda_1^*\right) Q^* \left|Q^*\right|. \tag{B.2}$$

where the non-dimensional loss parameter, λ_0^*, is

$$\lambda_0^* = \lambda_0 \frac{ga}{(c\omega)^2}, \tag{B.3}$$

and represents the non-dimensional bottom drag and the exit separation effect.

The model calculates the average extractable power for electricity generation for various magnitudes of turbine drag and losses within the channel. The numerical solution obtained in Section 3.1.2, when losses where neglected, may be conveniently scaled to provide a solution for the case of including losses. The general form of both equations is

$$\frac{dQ^*}{dt^*} = \cos t^* - \zeta_{Bay}^* - \lambda^* Q^* \left| Q^* \right|. \tag{B.4}$$

where $\lambda^* = \lambda_0^* + \lambda_1^*$ for both scenarios.

Appendix C – Helmholtz Frequency

The spike in power that is apparent in Figure 3.2 as β approaches unity may be explained by analyzing the natural frequency of the bay, ω_n. We will show that the tidal frequency is equal to the natural frequency, or Helmholtz frequency, of the bay when $\beta = 1$.

A channel linking a bay to the open ocean is analogous to a viscously damped forced vibration problem (VDFVP) if the damping coefficient is assumed to be linearly proportional to the flow rate. Vibration theory states that the natural frequency of a VDFVP is calculated by assuming that the damping term has a negligible impact on the frequency, and is therefore described by the homogeneous solution [26].

Continuity states that

$$\frac{dQ}{dt} = A\frac{d^2\zeta_{Bay}}{dt^2}. \tag{C.1}$$

Assuming negligible drag losses, the homogenous form of the governing equation (2.18) is

$$cA\frac{d^2\zeta_{bay}}{dt^2} + g\zeta_{bay} = 0. \tag{C.2}$$

Vibration theory states that the natural frequency of the bay system is then

$$\omega_n = \sqrt{\frac{g}{cA}}\,. \tag{C.3}$$

Substituting $\beta = g/cA\omega^2$ into (D.3), the natural frequency is expressed as a function of the tidal frequency as

$$\omega_n^2 = \beta\omega^2\,. \tag{C.4}$$

It is apparent from (D.4) that when $\beta = 1$, the tides are oscillating at the same frequency as the natural frequency of the bay. This explains why the amplitude of vibration in the system becomes very large as the bay geometry term approaches one.